RESEARCH ARTICLE

Targeting Chromatin Regulators Inhibits Leukemogenic Gene Expression in *NPM1* Mutant Leukemia

Michael W.M. Kühn[1,2], Evelyn Song[1], Zhaohui Feng[1], Amit Sinha[1], Chun-Wei Chen[1], Aniruddha J. Deshpande[1], Monica Cusan[1], Noushin Farnoud[1], Annalisa Mupo[3], Carolyn Grove[4,5], Richard Koche[1], James E. Bradner[6], Elisa de Stanchina[7], George S. Vassiliou[3], Takayuki Hoshii[1], and Scott A. Armstrong[1,8]

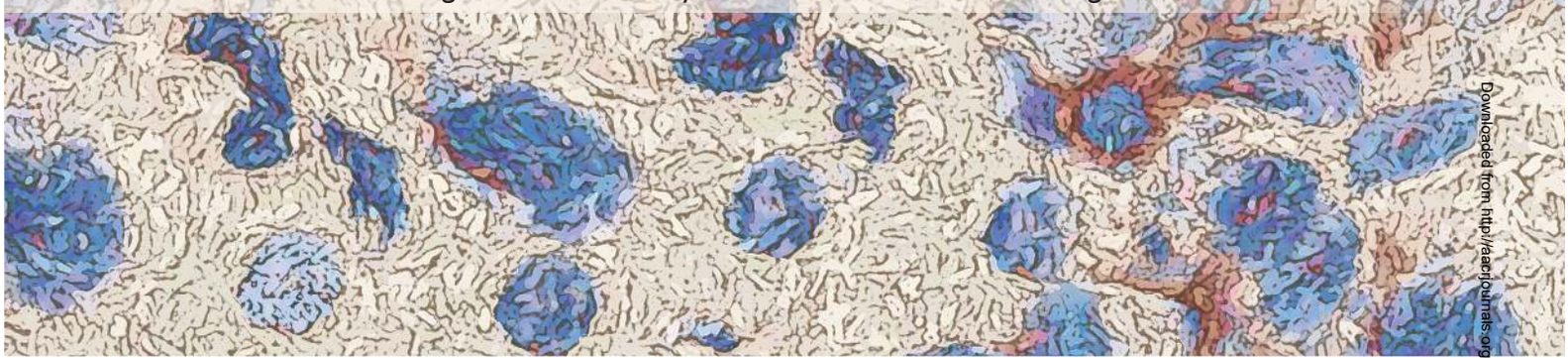

Downloaded from http://aacrjournals.org/cancerdiscovery/article-pdf/6/10/1166/1823310/1166.pdf by guest on 26 August 2022

ABSTRACT Homeobox (HOX) proteins and the receptor tyrosine kinase FLT3 are frequently highly expressed and mutated in acute myeloid leukemia (AML). Aberrant *HOX* expression is found in nearly all AMLs that harbor a mutation in the Nucleophosmin (*NPM1*) gene, and *FLT3* is concomitantly mutated in approximately 60% of these cases. Little is known about how mutant *NPM1* (*NPM1*^{mut}) cells maintain aberrant gene expression. Here, we demonstrate that the histone modifiers MLL1 and DOT1L control *HOX* and *FLT3* expression and differentiation in *NPM1*^{mut} AML. Using a CRISPR/Cas9 genome editing domain screen, we show *NPM1*^{mut} AML to be exceptionally dependent on the menin binding site in MLL1. Pharmacologic small-molecule inhibition of the menin–MLL1 protein interaction had profound antileukemic activity in human and murine models of *NPM1*^{mut} AML. Combined pharmacologic inhibition of menin–MLL1 and DOT1L resulted in dramatic suppression of *HOX* and *FLT3* expression, induction of differentiation, and superior activity against *NPM1*^{mut} leukemia.

SIGNIFICANCE: MLL1 and DOT1L are chromatin regulators that control *HOX, MEIS1,* and *FLT3* expression and are therapeutic targets in *NPM1*^{mut} AML. Combinatorial small-molecule inhibition has synergistic on-target activity and constitutes a novel therapeutic concept for this common AML subtype. *Cancer Discov; 6(10); 1166–81. ©2016 AACR.*

See related commentary by Hourigan and Aplan, p. 1087.

[1]Cancer Biology and Genetics Program, Memorial Sloan Kettering Cancer Center, New York, New York. [2]Department of Medicine III, University Medical Center, Johannes Gutenberg University, Mainz, Germany. [3]Wellcome Trust Sanger Institute, Hinxton, Cambridge, United Kingdom. [4]Department of Haematology, PathWest/Sir Charles Gairdner Hospital, Nedlands, Western Australia, Australia. [5]School of Pathology and Laboratory Medicine, University of Western Australia, Crawley, Western Australia, Australia. [6]Department of Medical Oncology, Dana-Farber Cancer Institute, Harvard Medical School, Boston, Massachusetts. [7]Antitumor Assessment Facility, Memorial Sloan Kettering Cancer Center, New York, New York. [8]Department of Pediatric Oncology, Dana-Farber Cancer Institute, and Division of Hematology/Oncology, Boston Children's Hospital, Harvard Medical School, Boston, Massachusetts.

Note: Supplementary data for this article are available at Cancer Discovery Online (http://cancerdiscovery.aacrjournals.org/).

Corresponding Author: Scott A. Armstrong, Dana-Farber Cancer Institute, Harvard Medical School, 450 Brookline Avenue, Boston, MA 02215. Phone: 617-632-3644; Fax: 617-632-4367; E-mail: scott_armstrong@dfci.harvard.edu

doi: 10.1158/2159-8290.CD-16-0237

©2016 American Association for Cancer Research.

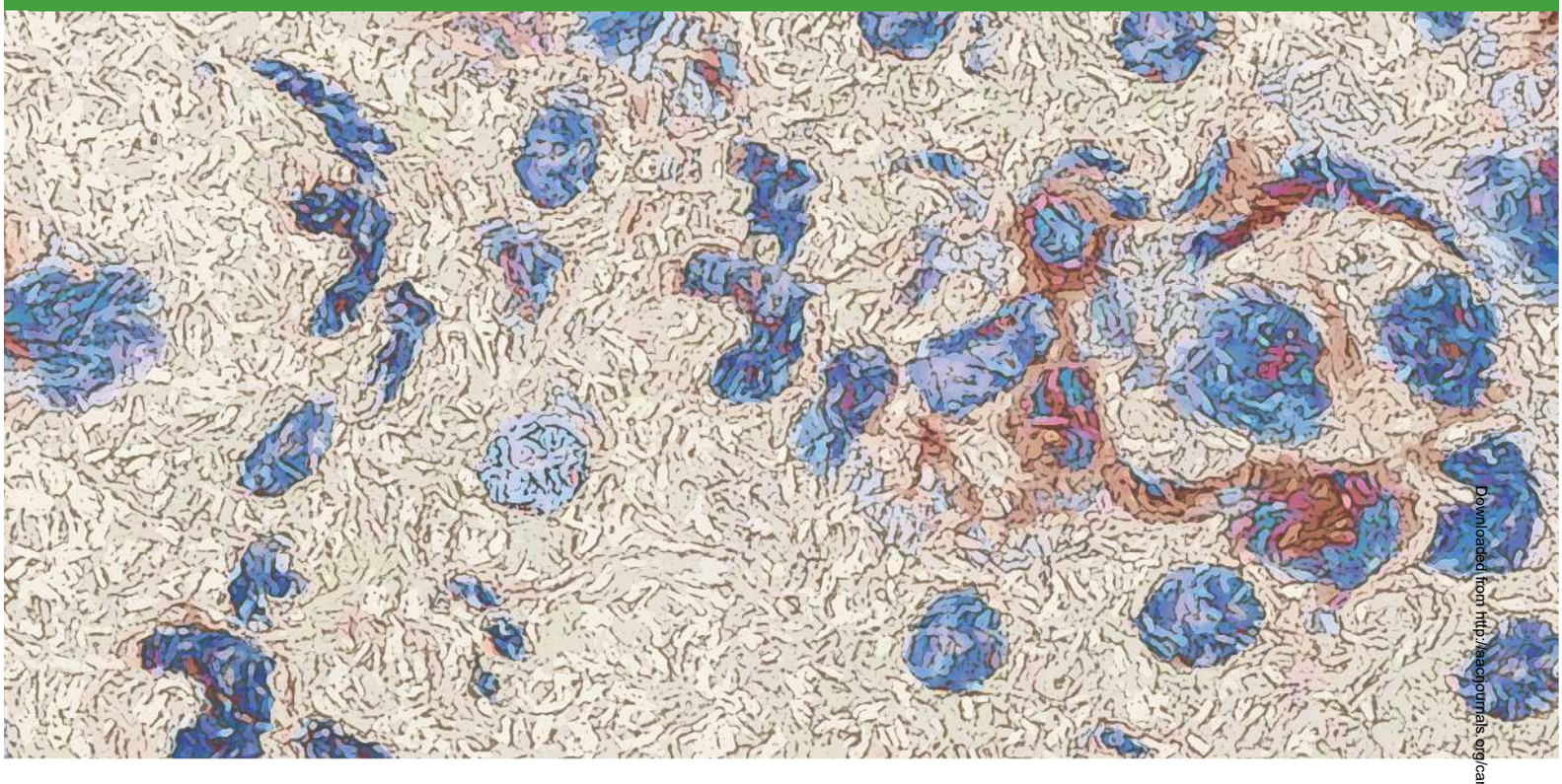

Downloaded from http://aacrjournals.org/cancerdiscovery/article-pdf/6/10/1166/1823310/1166.pdf by guest on 26 August 2022

INTRODUCTION

The clustered *HOX* genes are a highly conserved family of transcription factors that are expressed during early development and hematopoiesis (1–3). Specific members of the *HOXA* and *HOXB* cluster are required to maintain self-renewal properties of hematopoietic stem cells (HSC; ref. 3). Aberrant *HOX* gene expression is also a common feature of acute leukemias and can be activated by various oncogenes in murine leukemia models (3, 4). These genes are believed to play an important role during leukemogenesis because ectopic expression of specific members of the *HOX* cluster induces leukemic transformation of murine HSCs (5). In human acute myeloid leukemia (AML), aberrant *HOX* expression is found in 40% to 60% of the cases, whereas the specific *HOX* expression pattern is heterogeneous and has been used to categorize AML cases into four main groups that correlate with the presence of specific molecular markers (4). Simultaneous *HOXA* and *HOXB* cluster expression is most commonly found and frequently associated with the presence of an *NPM1* mutation (4, 6, 7), one of the two most frequently mutated genes in AML (8).

Mutant *NPM1* co-occurs often with other mutations in AML, most commonly in the *FLT3* (60%) and/or the *DNMT3A* (50%) genes (9–11). Although *NPM1*^{mut} AML lacking an internal tandem duplication (ITD) in the *FLT3* gene is considered a relatively favorable genotype with overall survival rates of up to 60% in younger patients, the presence of a concurrent *FLT3*-ITD converts this genotype into a less favorable category (9, 11, 12). The receptor tyrosine kinase *FLT3* is of particular interest because (a) its mutation status is used as a prognostic indicator guiding treatment decisions in patients with AML and (b) it represents a molecular target for small-molecule inhibition. Clinical trials have shown activity of several FLT3 inhibitors against *FLT3*-mutated AML, but resistance occurred frequently and quickly (13). Currently, less than 50% of the (younger) patients with *NPM1*^{mut} *FLT3*-ITD–positive AML achieve a sustainable remission, and survival rates of patients with *NPM1*^{mut} AML >65 years of age are even more dismal (11, 14). These data highlight the need for novel therapeutic concepts, which may be less toxic and more efficacious.

NPM1 is an intracellular chaperone protein implicated in multiple cellular processes, such as proliferation and ribosome and nucleosome assembly (15, 16), but it has remained elusive how *NPM1* mutations initiate and maintain AML, thus hindering the development of targeted therapeutic approaches. It is also unknown what mechanisms drive aberrant *HOX* gene expression in these leukemias. Our current knowledge of *HOX* gene regulation in leukemias has so far come from studies of *MLL1*-rearranged leukemias. In these leukemias, chromosomal translocations cause a fusion of the mixed-lineage leukemia gene (*MLL1*, also known as *MLL* or *KMT2A*) with one of more than 60 different fusion partners, resulting in the formation of an oncogenic fusion protein (17). *MLL1*-rearranged leukemias exhibit aberrant *HOXA*-cluster expression as a consequence of chromatin binding of the MLL1-fusion complex (18), which in turn requires the association with at least two other proteins, menin and LEDGF. Whereas menin facilitates LEDGF binding to the complex, the latter directly mediates chromatin binding of MLL1 (19, 20). Menin, the protein encoded by the multiple endocrine neoplasia 1 gene (*MEN1*), is of particular interest, as it is required

by MLL1-fusion proteins for transformation and has been shown to be therapeutically targetable. Recently developed inhibitors of the menin–MLL1 interaction were demonstrated to have antileukemic activity in preclinical *MLL1*-rearranged leukemia models (21, 22). Although *NPM1*^{mut} AML lack MLL1-fusion proteins, studies of conditional *MLL1* knockout mice have shown that wild-type *MLL1* (WT-*MLL1*) is required for maintenance of *HOX* gene expression during normal hematopoiesis (23, 24). In addition, it has been shown that WT-*MLL1* also requires the interaction with menin to maintain *HOX* expression and self-renewal properties of hematopoietic progenitors (25, 26).

The histone 3 lysine 79 (H3K79) methyltransferase DOT1L is another protein of therapeutic interest involved in *HOXA* cluster regulation of *MLL1*-rearranged leukemias (27–29). DOT1L is believed to be recruited to promoters of *HOXA* cluster genes via the MLL1-fusion partner that is commonly part of the DOT1L binding complex (30). Small-molecule inhibitors of DOT1L were proven to have activity against preclinical models of *MLL1*-rearranged leukemias (31, 32), and are currently being tested in a clinical trial (NCT01684150) with promising first results (33). DOT1L has also been linked to *HOX* gene control during normal hematopoiesis. Higher states of H3K79 methylation, such as dimethylation and trimethylation (me2 and me3) at the *Hox* locus, are associated with high expression levels of these genes in lineage$^-$, *Sca*1$^+$, c-*Kit*$^+$ (LSK) murine hematopoietic progenitors and are converted into monomethylation (me1) as these cells mature into more committed progenitors lacking *Hox* expression (28). Whether *Hoxb*-cluster expression in LSKs is also associated with H3K79me2 and me3 is unknown to date.

We hypothesized that aberrant *HOX* and *MEIS1* gene expression in *NPM1*^{mut} AML might be driven by similar mechanisms that control these genes in normal HSCs and that high expression of *FLT3*, a reported downstream target of *MEIS1*, is indirectly driven via elevated *MEIS1* transcript levels. In the current study, we use CRISPR/Cas9 genome editing and small-molecule inhibition to identify the chromatin regulators MLL1 and DOT1L as therapeutic targets that control *HOX, MEIS1,* and *FLT3* expression and differentiation in *NPM1*^{mut} leukemia.

RESULTS

CRISPR/Cas9 Mutagenesis Demonstrates a Requirement for MLL1 and Menin Binding in *NPM1*^{mut} Leukemia

Because MLL1 has been shown to regulate critical gene expression programs, including *HOX* gene expression in normal hematopoiesis and *MLL1*-rearranged AML, we hypothesized that it might also regulate *HOX* gene expression in other settings. As an initial assessment, we used an approach recently developed by Shi and colleagues that uses genome editing across exons encoding specific protein domains to determine the functional relevance of a given domain and the suitability for drug development (34). To assess potential dependencies of *NPM1*^{mut} AML on specific protein domains of MLL1 and its most similar family member MLL2 (also known as KMT2B), we designed a negative selection CRISPR/Cas9 screen interrogating multiple domains of both proteins (Supplementary Tables S1 and S2). We generated a tetracycline-inducible Cas9-expressing OCI-AML3 cell line (OCI-AML3-pCW-Cas9, Fig. 1A and B) as OCI-AML3 is the only commercially available human AML cell line harboring *NPM1*^{mut}. After transduction with 2 to 4 GFP$^+$ single-guide RNAs (sgRNA) interrogating each domain, Cas9 was induced and the GFP$^+$/GFP$^-$ ratio assessed over a period of 15 days. Cells expressing sgRNAs targeting exon 1 that encodes the menin–LEDGF binding motif of MLL1 as defined by Huang and colleagues (35) were rapidly outcompeted by their GFP$^-$ counterparts (Fig. 1C and D; fold change of GFP$^+$ d0/d15 up to 100). Similar results were obtained for one of two sgRNAs targeting the first exon of *RPA3*, a gene required for DNA replication that is used as a positive control, whereas there was no difference in GFP expression over time in an empty-vector control guide (Fig. 1C). Having found selection against the sgRNAs targeting the menin–LEDGF binding motif, we performed SURVEYOR assays of sgRNAs targeting the menin–LEDGF binding motif and the N-HINGE-LOOP motif. The latter is located just 5′ from the menin–LEDGF locus but is considered as nonessential for the menin–MLL1 interaction and showed less negative selection in our screen. We detected indel mutations at day 3 for both sgRNAs but at day 9 only for the N-HINGE-LOOP sgRNA (Supplementary Fig. S1). These results are consistent with the selection data from our screen that demonstrate outcompeting of the cells transduced with the menin–LEDGF sgRNAs. Interestingly, sgRNAs targeting exons that encode the CXXC domain of MLL1, also known to be involved in chromatin binding and required for MLL1-fusion leukemia, were also selected against in our screen (Fig. 1C and E; refs. 36, 37). Of interest, no significant phenotype was observed for sgRNAs targeting the C-terminal SET domain of MLL1 (Fig. 1C). We validated these findings by performing a second screen using another independently engineered OCI-AML3-pCW-Cas9 clone (OCI-AML3-pCW-Cas9-C8; Fig. 1B) and obtained similar results, with sgRNAs targeting the menin–LEDGF binding motif again being the top hit (Supplementary Fig. S2A and S2B). We found no significant negative selection for any sgRNAs that interrogated the MLL2 protein domains (Fig. 1F). These data suggest that the menin–LEDGF binding motif of MLL1 but not MLL2 is required for *NPM1*^{mut} AML.

Pharmacologic Disruption of the Menin–MLL1 Interaction Suppresses *HOX*, *MEIS1*, and *FLT3* Expression and Induces *NPM1*^{mut} AML Differentiation

The genetic data presented above indicate that the menin–MLL1 interaction might be a therapeutic target in *NPM1*^{mut} AML. We therefore assessed whether recently developed small-molecule inhibitors of the menin–MLL1 interaction might influence proliferation and gene expression in *NPM1*^{mut} AML cells. First, we assessed the effects of MI-2-2, a small-molecule inhibitor of this protein interaction in the human *NPM1*^{mut} AML cell line OCI-AML3 (21). We observed a profound dose-dependent reduction in cell proliferation that was even more pronounced than in the *MLL1*-rearranged MOLM13 cells that served as a positive control (Fig. 2A). The HL60 AML cells lacking an *NPM1*^{mut} or MLL1 fusion showed only a mild cell growth–inhibitory effect at higher doses (Fig. 2A). During the work on this study, MI-503, a novel menin–MLL1 inhibitor, was described (22) that was

Downloaded from http://aacrjournals.org/cancerdiscovery/article-pdf/6/10/1166/1823310/1166.pdf by guest on 26 August 2022

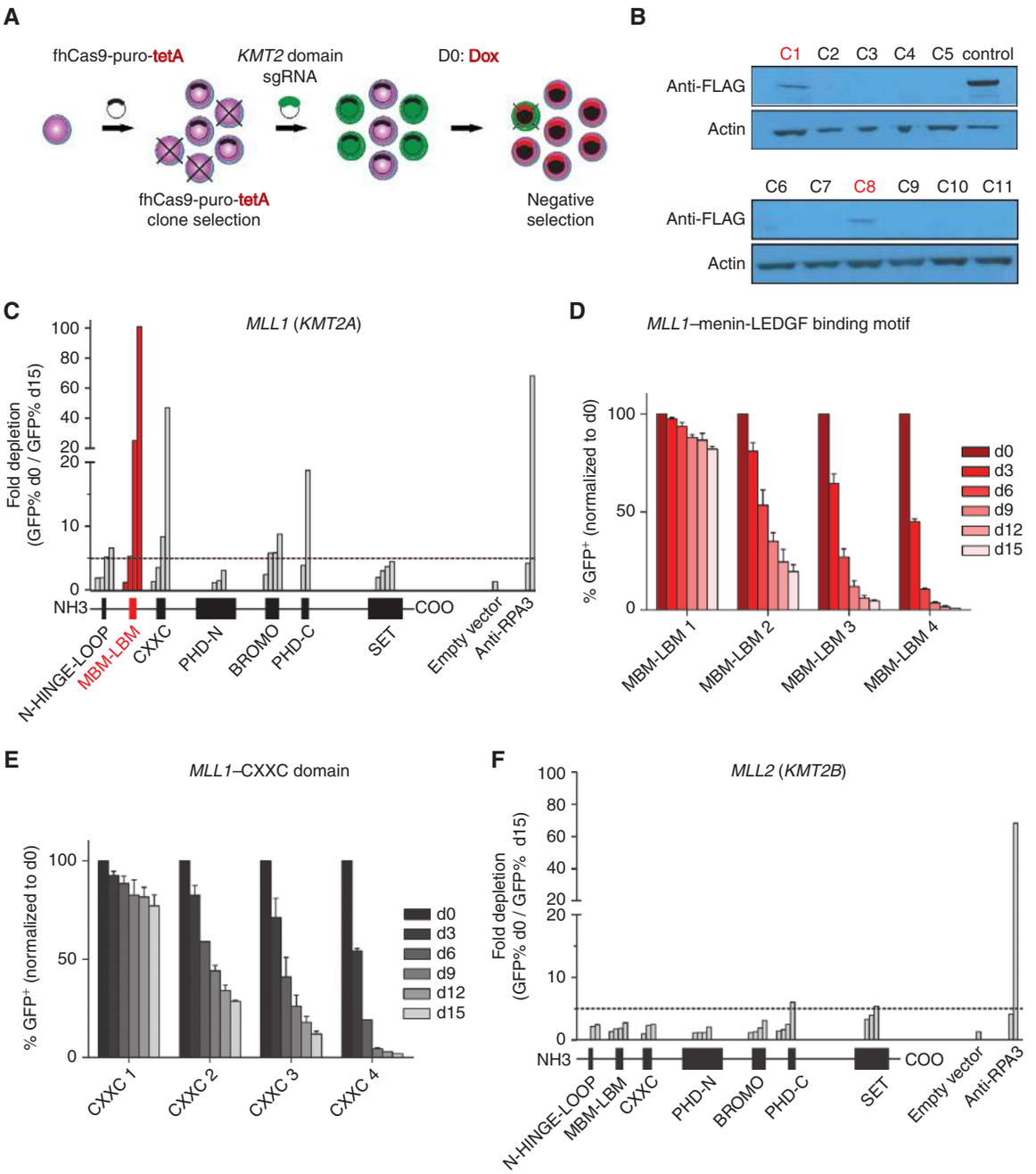

Figure 1. CRISPR/Cas9 mutagenesis of exons targeting MLL protein domains in *NPM1*^{mut} AML cells. **A,** experimental strategy for CRISPR/Cas9-negative selection screening: Engineering a clonal *NPM1*^{mut} OCI-AML3 cell line that expresses a FLAG-tagged human codon-optimized Cas9 (fhCas9) vector containing a puro resistance gene (puro) and tetracycline-inducible transcriptional activator (tetA). GFP reporters of sgRNA constructs were used to track sgRNA negative selection after doxycycline induction of Cas9 (D0, day 0; DOX, doxycycline). **B,** immunoblotting for FLAG-tagged hCas9 after doxycycline treatment in 11 OCI-AML3-Cas9 single-cell clones. C1 and C8 clones were selected for two independent screens of *MLL1* and *MLL2*. **C** and **F,** summary of negative selection experiments with sgRNAs targeting exons encoding specific MLL1 and MLL2 protein domains. Negative selection is plotted as the fold depletion of GFP$^+$ cells (d0 GFP% divided by d15 GFP%) during 18 days in culture. Each bar represents an independent sgRNA. The location of each sgRNA relative to the MLL1 or MLL2 protein is indicated along the *x* axis. The dashed line indicates a 5-fold change. The data shown are the mean value of two independent replicates. Empty-vector and anti-RPA3 sgRNA represent negative and positive controls. **D** and **E,** negative selection competition assay that plots the percentage of GFP$^+$ cells over time following transduction of OCI-AML3-Cas9 with the indicated sgRNAs. GFP$^+$ percentage is normalized to the day 0 measurement following doxycycline induction of Cas9 (3 days after sgRNA transduction). N-HINGE-LOOP, N-terminal hinge loop of the menin-LEDGF binding motif lacking many specific interactions; MBM-LBM, N-terminal fragment of MLL1 containing the menin and the LEDGF binding motif (as defined in ref. 35); CXXC, CXXC-type zink finger domain; PHD-N, N-terminal plant homeodomains; BROMO, bromodomain; PHD-C, C-terminal plant homeodomain; SET, SET domain. Data shown in **C** to **F** represent mean of biological duplicates.

Downloaded from http://aacrjournals.org/cancerdiscovery/article-pdf/6/10/1166/1823310/1166.pdf by guest on 26 August 2022

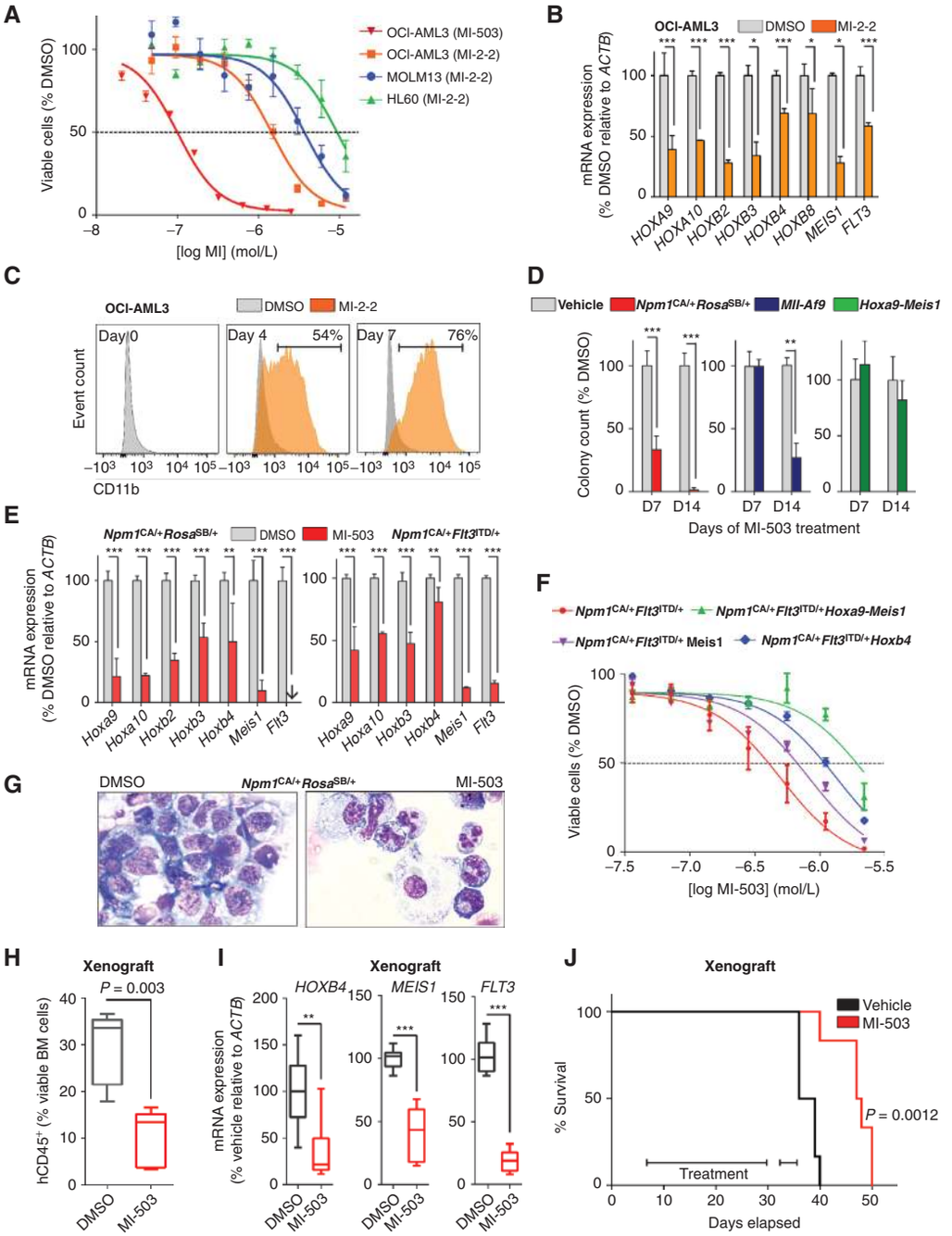

Figure 2. Effects of menin–MLL11-i in human and murine *NPM1*^{mut} leukemia cells *in vitro* and *in vivo*. **A,** dose–response curves from cell viability assays after 11 days of MI-2-2 or MI-503 treatment. **B,** *HOX* gene expression in the human OCI-AML3 cells following 4 days of MI-2-2 (12 μmol/L) treatment. **C,** cell differentiation upon menin–MLL1-i (MI-2-2: 12 μmol/L) as determined by CD11b expression in OCI-AML3 cells (at days 0, 4, and 7 of treatment). **D,** MI-503 (2.5 μmol/L) treatment of murine *Npm1*$^{CA/+}$*Rosa*$^{SB/+}$, *MII-Af9*, and *Hoxa9-Meis1*–transformed cells in colony-forming assays assessed on day 7 and day 14 of treatment. **E,** gene expression in murine *Npm1*$^{CA/+}$*Flt3*$^{ITD/+}$ and *Npm1*$^{CA/+}$*Rosa*$^{SB/+}$ cells assessed on day 4 of MI-503 treatment (2.5 μmol/L). **F,** dose–response curves from cell viability assays after 11 days of MI-503 treatment comparing *Npm1*$^{CA/+}$*Flt3*$^{ITD/+}$ cells versus *Npm1*$^{CA/+}$*Flt3*$^{ITD/+}$ cells overexpressing *Hoxb4*, *Meis1*, or *Hoxa9-Meis1*. **G,** morphologic changes consistent with granulocytic/monocytic differentiation in murine *Npm1*$^{CA/+}$*Rosa*$^{SB/+}$ cells after 7 days of MI-503 (2.5 μmol/L) treatment. **H,** assessment of leukemia burden in an OCI-AML3 xenotransplantation model after 7 to 12 days of MI-503 *in vivo* treatment as determined by human CD45–positive cells in the murine bone marrow. **I,** gene expression changes after 12 days of MI-503 (50 mg/kg b.i.d. IP) *in vivo* treatment. **J,** survival of OCI-AML3 xenograft mice ($n = 6$ mice/group) treated with MI-503 (50 mg/kg bid IP). Data represent averages of two independent experiments, each performed in three replicates (**A, B, C, D, E, F**) except for the dose response to MI-503 (red curve in **A**) that was once performed (in three replicates) to independently confirm sensitivity to menin–MLL1-i. Error bars represent SEM. The whiskers of box plots (**H** and **I**) represent minimal and maximal values of 5 (**H**) and 3 (**I**) mice per group, the box represents the SEM, the line represents the median.

Downloaded from http://aacrjournals.org/cancerdiscovery/article-pdf/6/10/1166/1823310/1166.pdf by guest on 26 August 2022

synthesized by re-engineering the molecular scaffold of MI-2-2, resulting in enhanced drug-like properties and *in vivo* utility. To compare the two compounds and to define equivalent growth-inhibitory concentrations, we generated dose–response curves for both inhibitors, confirming the higher potency of MI-503 over MI-2-2 (Fig. 2A and Supplementary Fig. S3). MI-503 was used for most of the subsequent experiments.

We next assessed gene expression in the *NPM1*^{mut} AML cells and found a significant downregulation of *HOXA* cluster, *HOXB* cluster, and *MEIS1* gene expression upon 4 days of treatment with MI-2-2 (Fig. 2B). Of these, *MEIS1* appeared to be the most profoundly suppressed gene. This finding led us to explore a possible effect of menin–MLL1 inhibition (menin–MLL1-i) on *FLT3* expression, as *FLT3* is a reported downstream target of *MEIS1* (38). In fact, *FLT3* transcript levels were also substantially and highly significantly suppressed upon MI-2-2 treatment (Fig. 2B). To characterize the effects of pharmacologic menin–MLL1-i in more detail, we assessed apoptosis and differentiation following MI-2-2 treatment. Whereas induction of apoptosis was moderate (Supplementary Fig. S4), we observed profound differentiation following menin–MLL1-i, as reflected by an increase in CD11b expression over time as determined by flow cytometry [Fig. 2C; vehicle: 1.3%; MI-2-2: 76% (mean expression, day 7 of treatment)].

Next, we sought to validate our findings from the human OCI-AML3 cells on two independent murine conditional knock-in models of *NPM1*^{mut} leukemia. One of the leukemias is engineered to possess both an *Npm1* mutation and a *Flt3*-ITD (*Npm1*$^{CA/+}$*Flt3*$^{ITD/+}$), whereas in the other model, secondary mutations were induced through use of a sleeping beauty transposon system (*Npm1*$^{CA/+}$*Rosa*$^{SB/+}$; refs. 39, 40). For *in vitro* drug testing, leukemic blasts were harvested from moribund primarily transplanted mice and cultured. As *Npm1*$^{CA/+}$*Rosa*$^{SB/+}$ cells did not grow in liquid culture medium but in methylcellulose only, we performed MI-503 treatment of these cells in colony-forming assays. Treatment for 7 and 14 days, respectively, resulted in a profound inhibitory effect on colony-forming potential in the *Npm1*$^{CA/+}$*Rosa*$^{SB/+}$ cells as well as in *Mll-Af9* leukemia cells that served as a positive control, whereas *Hoxa9-Meis1*–transformed cells were unaffected (Fig. 2D). Similar results were obtained for *Npm1*$^{CA/+}$*Flt3*$^{ITD/+}$ cells that grow in liquid culture. These leukemias exhibited profound sensitivity to MI-503 and MI-2-2 treatment in a dose-dependent manner, which was even more pronounced than in the *Mll-Af9* leukemia cells (Supplementary Fig. S3).

Next, we assessed the effects of MI-503 on *Hox* gene expression in both murine *Npm1*^{mut} leukemia models. Although baseline expression levels of individual *Hox* genes differed between the two murine leukemias, with for example lack of *Hoxb2* expression in *Npm1*$^{CA/+}$*Flt3*$^{ITD/+}$ cells, we observed substantial suppression of *Hoxa* cluster and *Hoxb* cluster genes as well as *Meis1*. Of these, *Meis1* was the most profoundly suppressed gene and again accompanied by substantial downregulation of global *Flt3* transcript levels (Fig. 2E). To further explore whether the antiproliferative effects of MI-503 are causally related to *Hox* suppression in these leukemias, we expressed *Meis1, Hoxb4,* and *Hoxa9-Meis1* ectopically in the *Npm1*$^{CA/+}$*Flt3*$^{ITD/+}$ murine leukemia cells. Of interest, all three scenarios rescued the *Npm1*$^{CA/+}$*Flt3*$^{ITD/+}$ cells from the menin–MLL1-i–mediated antiproliferative effect when exposed to MI-503 treatment for 11 days, as reflected by a shift of the dose–response curves toward higher concentrations and increased IC_{50} values (Fig. 2F).

As changes in *Hox* gene expression were followed by myeloid differentiation in the human cells, we then determined whether MI-503 also induces differentiation in the murine leukemias. In fact, cytologic analysis of both *Npm1*$^{CA/+}$*Rosa*$^{SB/+}$ and *Npm1*$^{CA/+}$*Flt3*$^{ITD/+}$ cells revealed morphologic changes consistent with substantial myelo-monocytic differentiation (Fig. 2G and Supplementary Fig. S5).

We next sought to investigate the therapeutic effects of menin–MLL1-i on leukemia burden *in vivo* using a disseminated human OCI-AML3 xenotransplantation model. OCI-AML3 cells were transplanted into NOD.*Cg-Prkdc*^{scid}*Il2rg*^{tm1Wjl}/SzJ (NSG) mice via tail-vein injection, and MI-503 treatment was initiated 7 days later. Animals were sacrificed after 7 (n = 2 per group) and 12 days (n = 3 per group) of MI-503 treatment [50 mg/kg twice daily (b.i.d.) by intraperitoneal injection (IP)]. Leukemia burden, as defined by the percentage of bone marrow cells expressing human CD45, was significantly reduced within the treated animal group compared with vehicle controls (Fig. 2H). To assess effects of MI-503 on gene expression *in vivo,* we analyzed sorted human CD45-positive bone marrow cells harvested from these animals for *HOXB4, MEIS1,* and *FLT3.* Twelve days of treatment resulted in dramatic suppression of these genes in the treated versus vehicle control animals (Fig. 2I).

We then explored the effects of MI-503 treatment on survival in the OCI-AML3 xenotransplantation model in a separate experiment. Treatment was initiated 7 days after transplantation at 50 mg/kg bid IP and continued for a total of 26 days excluding a 3-day break to allow recovery from local irritation at the injection site. MI-503 treatment resulted in a highly significant survival advantage compared with vehicle control animals (Fig. 2J; $P = 0.0012$; increase in median survival: 21%). Next, we sought to validate these findings in a murine model of *NPM1*^{mut} leukemia. Mice transplanted with secondary *Npm1*$^{CA/+}$*Rosa*$^{SB/+}$ leukemia cells were treated for 10 days with MI-503 versus vehicle control. Despite the aggressive character of this leukemia, with a disease latency of only 2 to 3 weeks, MI-503 significantly prolonged survival of leukemic animals (Supplementary Fig. S6; $P = 0.0045$, increase in median survival: 31%). These data indicate that therapeutic menin–MLL1-i reverses a *HOX* gene–dominated leukemogenic gene expression program in *NPM1*^{mut} leukemias *in vitro* and *in vivo*, thereby releasing the differentiation block in these cells and ultimately resulting in prolonged survival of mice suffering from *NPM1*^{mut} AML.

MI-503 Treatment Depletes Menin from *HOX* and *MEIS1* Loci in *NPM1*^{mut} Leukemias

Menin associates with MLL1 at *HOXA* and *MEIS1* promoters (19), and pharmacologic interruption of the menin–MLL1 interaction diminishes menin occupancy at the *HOXA* locus in *MLL1*-rearranged leukemias (41). We assessed the abundance of menin at *HOXA, HOXB,* and *MEIS1* loci in the human *NPM1*^{mut} leukemia cell line before and after pharmacologic menin–MLL1-i. Chromatin immunoprecipitation (ChIP) of menin followed by qPCR demonstrated the presence of menin at expressed *HOXA, HOXB,* and *MEIS1* gene loci, and menin was depleted from most of these loci after

Downloaded from http://aacrjournals.org/cancerdiscovery/article-pdf/6/10/1166/1823310/1166.pdf by guest on 26 August 2022

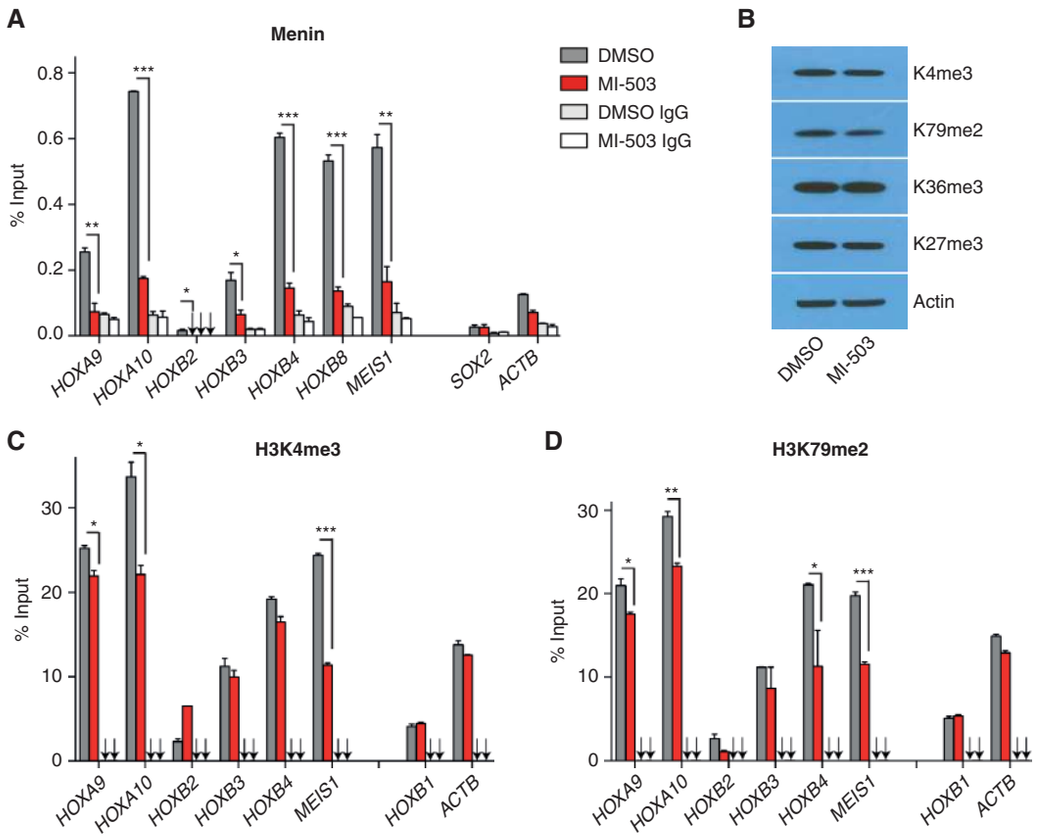

Figure 3. Menin–MLL1-i depletes menin, H3K4me3, and H3K79me2 at *HOX* and *MEIS1* gene loci in OCI-AML3 cells. **A,** relative enrichment of menin at selected *HOXA*, *HOXB*, and *MEIS1* gene loci in OCI-AML3 cells upon 5 days of MI-503 (2.5 μmol/L) treatment compared with drug vehicle as assessed by ChIP-PCR. **B,** immunoblotting of indicated histone marks following 4 days of MI-503 treatment (2.5 μmol/L). **C** and **D,** H3K4me3 and H3K79me2 enrichment across the *HOX* gene locus and at *MEIS1* following 6 days of MI-503 treatment (2.5 μmol/L) versus DMSO. One representative experiment is shown, bar graphs represent averages of three replicates, arrows point to IgG control values, and error bars represent SEM. Results were confirmed in two additional independent experiments.

5 days of MI-503 treatment (Fig. 3A). Reduction of menin enrichment was particularly pronounced at the *MEIS1* locus, thereby correlating with findings from gene expression analysis (Figs. 2B and 3A).

Although we did not detect global changes of several chromatin marks upon menin–MLL1-i (Fig. 3B), we observed a locus-specific decrease of H3K4me3 at *HOX* and *MEIS1* loci (Fig. 3C), thus demonstrating the expected changes in histone methylation due to menin–MLL1-i. Somewhat unexpectedly, we also found a significant reduction of H3K79me2 at those loci (Fig. 3D). These data are consistent with decreased binding of the menin–MLL1 complex to *HOX* and *MEIS1* loci following pharmacologic menin–MLL1-i and also point to the H3K79 methyltransferase DOT1L as having a potential role in *HOX* gene regulation in *NPM1*^{mut} leukemia cells.

DOT1L Is Involved in *HOXA* and *HOXB* Cluster Regulation during Normal Hematopoiesis and in *NPM1*^{mut} Leukemia

The data described above suggest WT-MLL1 to be important for *HOX* gene control in *NPM1*^{mut} AML, and also implicate DOT1L in *HOX* gene regulation in this disease. Recent studies of benign murine hematopoiesis demonstrated that DOT1L is another chromatin regulator critical for *Hoxa*-cluster regulation in early hematopoietic progenitors, whereas its role in *Hoxb* cluster control is not well defined (28). To explore whether DOT1L might be involved in the control of *Hoxb*-cluster genes, we reanalyzed gene expression data from *Dot1l*$^{fl/fl}$ Mx1-Cre transgenic mice after polyinosinic–polycytidylic acid-induced excision compared with their normal counterparts (27). In fact, we found the anterior *Hoxb* cluster genes *Hoxb2* and *Hoxb4* to be significantly downregulated after homozygous deletion of *Dot1l* (Fig. 4A), whereas there was also a trend for *Hoxb3* that did not reach statistical significance. In addition, there was an association between high expression levels of early *Hoxb*-cluster genes and higher states of H3K79 methylation (H3K79me2 and me3) in normal murine LSKs (Fig. 4B) mimicking the H3K79 profile across the expressed *Hoxa* cluster genes in these cells. These findings extend the concept of DOT1L being critical for *Hoxa* cluster regulation during normal hematopoiesis to the *Hoxb* cluster, which together represent also the dominant expression pattern found in *NPM1*^{mut} leukemias.

Based on these findings, we assessed the effect of EPZ4777, a small-molecule DOT1L inhibitor in *NPM1*^{mut} leukemias. DOT1L-inhibition (DOT1L-i) led to a profound reduction in

Downloaded from http://aacrjournals.org/cancerdiscovery/article-pdf/6/10/1166/1823310/1166.pdf by guest on 26 August 2022

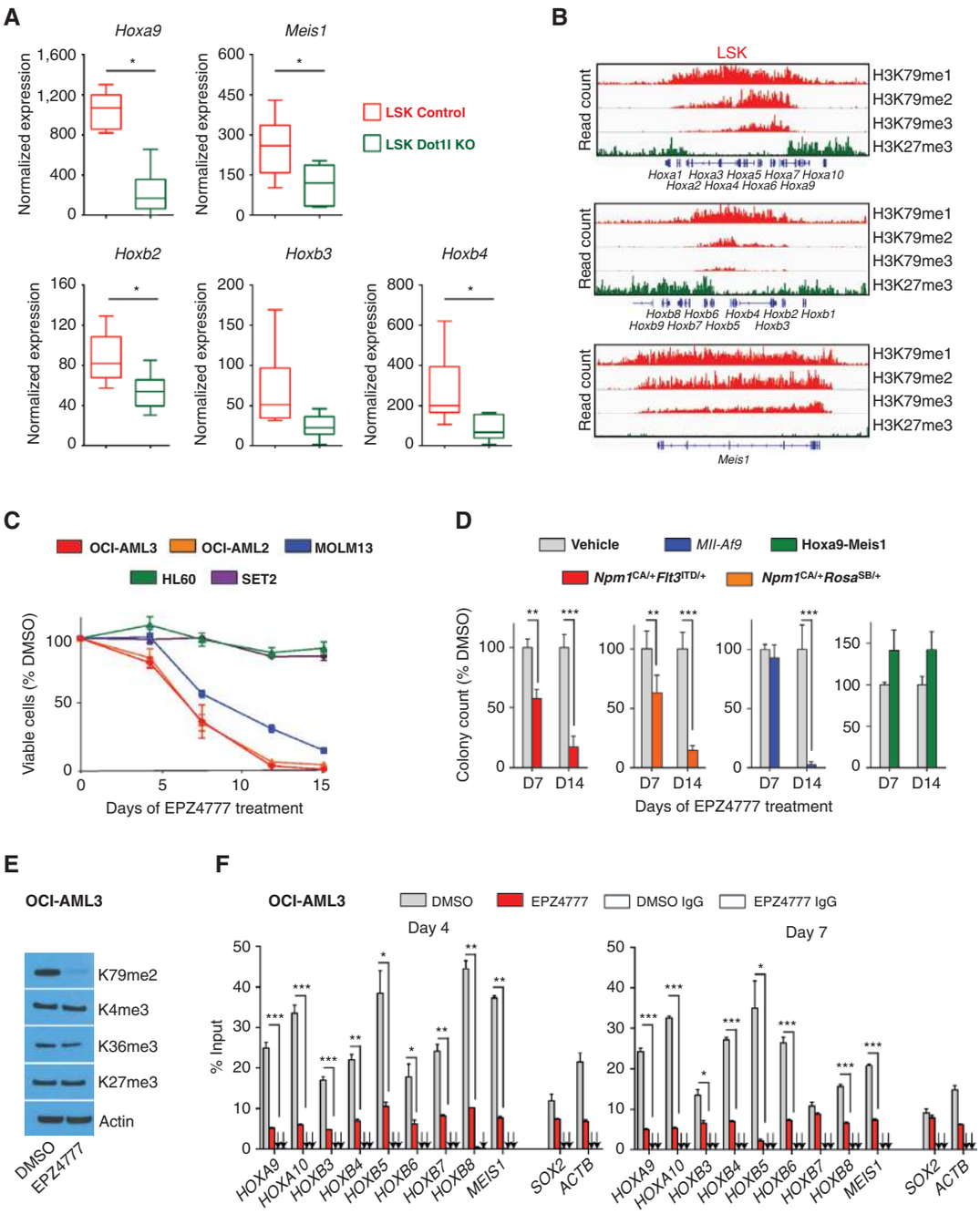

Figure 4. DOT1L is required for *HOXB*-cluster expression in early hematopoietic progenitors and a therapeutic target in *NPM1*^{mut} leukemia. **A,** expression of *Hoxa9, Meis1, Hoxb2, Hoxb3, and Hoxb4* in LSK cells sorted from *Dot1l*$^{fl/fl}$ or *Dot1l*$^{WT/WT}$ mice crossed with Mx1-Cre mice after 10 days of plpC treatment. **B,** representative profiles for ChIP-seq using anti-H3K79me1, H3K79me2, H3K79me3, and H3K27me3 antibodies in LSK cells at the *Hoxa* and *Hoxb* cluster. The *y* axis scale represents read density per million sequenced reads. **C,** growth of OCI-AML3, MOLM13, SET2, OCI-AML2, and HL60 cells exposed to EPZ4777 (10 μmol/L). Viable cells were counted and replated at equal cell numbers in fresh media with fresh compound every 3 to 4 days. Results were plotted as percentage of split-adjusted viable cells in the presence of EPZ4777 (10 μmol/L) and normalized to DMSO control. **D,** colony numbers of *Npm1*$^{CA/+}$*Flt3*$^{ITD/+}$, *Npm1*$^{CA/+}$*Rosa*$^{SB/+}$, *MII-Af9,* and *Hoxa9-Meis1* cells exposed to 10 μmol/L EPZ4777 and compared with DMSO vehicle control. Data were obtained at day 7 (D7), when viable cells were harvested and replated in fresh methylcellulose with fresh compound and at day 14 (D14) of treatment. **E,** immunoblotting of global histone marks in OCI-AML3 cells upon 4 days of EPZ4777 treatment (10 μmol/L). **F,** H3K79me2 levels across the *HOXA* and *HOXB* cluster locus and *MEIS1* in OCI-AML3 cells after 4 and 7 days of EPZ4777 (10 μmol/L) treatment and compared with DMSO control as assessed by ChIP-PCR. The box plots in **A** show normalized expression values of 6 mice per group. Whiskers represent minimal and maximal values, the box represents the SEM, and the line represents the median. Data in **C** and **D** represent averages of three independent experiments, each performed in three replicates. Error bars represent the SEM. For ChIP data in **F,** one representative experiment performed in three replicates is shown, arrows point to the IgG control values, and error bars represent the SEM. Results were confirmed in two additional independent experiments.

Downloaded from http://aacrjournals.org/cancerdiscovery/article-pdf/6/10/1166/1823310/1166.pdf by guest on 26 August 2022

cell proliferation and colony-forming potential in the human and both murine *NPM1*^{mut} leukemia models. Similar results were obtained for MLL1-fusion leukemias, whereas leukemias lacking an *NPM1* mutation or MLL1 fusion such as human HL60 cells and murine *Hoxa9-Meis1 in vitro*–transformed cells were unaffected (Fig. 4C and D). Antiproliferative effects of DOT1L-i in the human cells were preceded by global and *HOX* and *MEIS1* locus–specific reduction in H3K79me2 as determined by immunoblotting and ChIP-PCR, whereas global levels of other histone marks associated with transcriptional activation (H3K4me3, H3K36me3) and transcriptional repression (H3K27me2) were unchanged (Fig. 4E and F). As hypothesized, DOT1L-i resulted in significant repression of *HOX* genes in human and murine leukemia cells, although the pattern differed slightly among the models (Fig. 5A, left, and Fig. 5B). The murine leukemias exhibited significant suppression of *Hoxa, Hoxb,* and *Meis1* genes (Fig. 5B), whereas the *HOXB* cluster was suppressed in human cells, but the *HOXA* cluster was only mildly affected, as assessed by RNA sequencing (Fig. 5A, left). Of note, *MEIS1* was most profoundly downregulated across all *NPM1*^{mut} models. This finding was accompanied by dramatic *FLT3* suppression (Fig. 5A, left, and B). To control the results from the RNA-sequencing analysis for potential bias from standard normalization in the context of global transcriptional changes as they might occur with global changes of chromatin marks, we normalized on synthetic RNA spike-in controls as proposed by Loven and colleagues and compared the results to standard normalization (42). No difference of global transcription levels was noted (data not shown), indicating that global reduction of H3K79me2 is associated not with global transcriptional downregulation in these cells but with suppression of a smaller *HOX* dominated gene subset. As EPZ4777 treatment resulted in profound suppression of *Hox* cluster genes followed by substantial growth inhibition of *Npm1*^{mut} leukemia cells, we next assessed whether retroviral overexpression of *Hoxb4, Meis1,* or *Hoxa9-Meis1* influenced the treatment response to EPZ4777 of these leukemias. As demonstrated for menin–MLL1-i, ectopic expression of these genes abolished sensitivity of *Npm1*$^{CA/+}$*Flt3*$^{ITD/+}$ cells to DOT1L-i (Fig. 5C).

Because gene expression changes observed in response to EPZ4777 treatment were also consistent with cell differentiation (Fig. 5A, right), we next assessed the human *NPM1*^{mut} AML cells for differentiation following DOT1L-i. As expected, we observed a strong increase of CD11b expression as determined by flow cytometry and morphologic changes consistent with myeloid differentiation in the OCI-AML3 cells beginning at day 7 of treatment (Fig. 5D). *Npm1*$^{CA/+}$*Flt3*$^{ITD/+}$ and *Npm1*$^{CA/+}$*Rosa*$^{SB/+}$ cells also showed substantial monocytic cell differentiation after 14 days of pharmacologic DOT1L-i (Fig. 5E).

As *HOX* gene expression is associated with self-renewal properties, we next determined whether pharmacologic DOT1L-i inhibits *NPM1*^{mut} leukemia initiation in mice. Murine *Npm1*$^{CA/+}$*Rosa*$^{SB/+}$ leukemia cells were treated *ex vivo* with EPZ4777 or drug vehicle for 10 days, and equal numbers of viable cells were transplanted into sublethally irradiated recipient animals. A significant survival advantage was noted for the animals transplanted with treated cells compared with vehicle control in both *NPM1*^{mut} leukemia models (Fig. 5F and Supplementary Fig. S7), and animals transplanted with the EPZ4777-treated *Npm1*$^{CA/+}$*Rosa*$^{SB/+}$ leukemia cells had normal white blood cell (WBC) counts at disease onset of the vehicle control group (Fig. 5F–H). Similar results were obtained for the *Npm1*$^{CA/+}$*Flt3*$^{ITD/+}$ cells but with longer disease onset within the treated group (Supplementary Fig. S7). These data are therefore consistent with DOT1L participating in *HOX* gene regulation and differentiation control of *NPM1*^{mut} leukemia cells, thereby reprogramming these cells toward a state with substantially decreased leukemia-initiating and self-renewal properties.

DNMT3A Mutations Do Not Account for Sensitivity of *NPM1*^{mut} AML to DOT1L-i

In addition to the *NPM1* mutation, OCI-AML3 cells harbor a *DNMT3A* mutation (R882C), which has been linked to aberrant *HOX* expression in AML in some studies (4) but was attributed to concomitant *NPM1* mutations in others (43). To explore whether *DNMT3A* mutation status is associated with sensitivity to DOT1L-i, we included two additional cell lines with *DNMT3A* mutations in our study. Although the *JAK2*-mutated SET2 cells (which harbor the most common AML-associated *DNMT3A* mutation, R882H) did not show sensitivity to DOT1L-i, the OCI-AML2 cells (R635W reported in a single patient; ref. 44) were found to be tremendously sensitive (Fig. 4C). To understand these conflicting findings, we searched for other genetic factors potentially influencing sensitivity to EPZ4777 in the OCI-AML2 cells. Unexpectedly, RNA sequencing revealed the presence of an *MLL–AF6* fusion transcript with breakpoints that aligned to the common breakpoint cluster region typically affected in *MLL–AF6*-rearranged leukemias that was confirmed by breakpoint spanning RT-PCR (Supplementary Fig. S8A). Whereas conventional cytogenetic analysis confirmed the normal 11q23 loci as reported, we detected a *MLL1* split signal mapping to the derivative chromosome 1q using FISH (Supplementary Fig. S8B and S8C). These findings are consistent with a cryptic insertion of a functionally relevant *MLL–AF6* fusion into the derivative chromosome 1. Also, we found the typical MLL1 fusion–related gene signature with high-level *HOXA* expressions that were profoundly downregulated upon DOT1L-i but lack of *HOXB* cluster expression (Supplementary Fig. S9). Together, these data support a previous study reporting that DOT1L controls *HOXA* cluster expression also in MLL1-fusion leukemia with no apparent DOT1L-recruiting activity (such as *MLL–AF6*; ref. 45). However, whether *DNMT3A* mutations are associated with sensitivity to DOT1L-i remains to be fully determined.

Combinatorial Menin–MLL1-i and DOT1L-i Synergistically Suppresses *HOX*, *MEIS1*, and *FLT3* Expression and Induces Differentiation in *NPM1*^{mut} Leukemia

Our data are consistent with the menin–MLL1 interaction and DOT1L both being important regulators that control *HOX, MEIS1,* and *FLT3* expression in *NPM1*^{mut} AML. We therefore sought to investigate the effects of combinatorial menin–MLL1-i and DOT1L-i in the three models of *NPM1*^{mut} AML. Combinatorial drug treatment in liquid culture resulted in improved growth inhibition as reflected by a shift of the dose–response curve toward lower doses compared with each of the compounds alone in the human OCI-AML3 and the murine *Npm1*$^{CA/+}$*Flt3*$^{ITD/+}$ cells (Fig. 6A and B). Of note, significant drug synergism was demonstrated for both the

Downloaded from http://aacrjournals.org/cancerdiscovery/article-pdf/6/10/1166/1823310/1166.pdf by guest on 26 August 2022

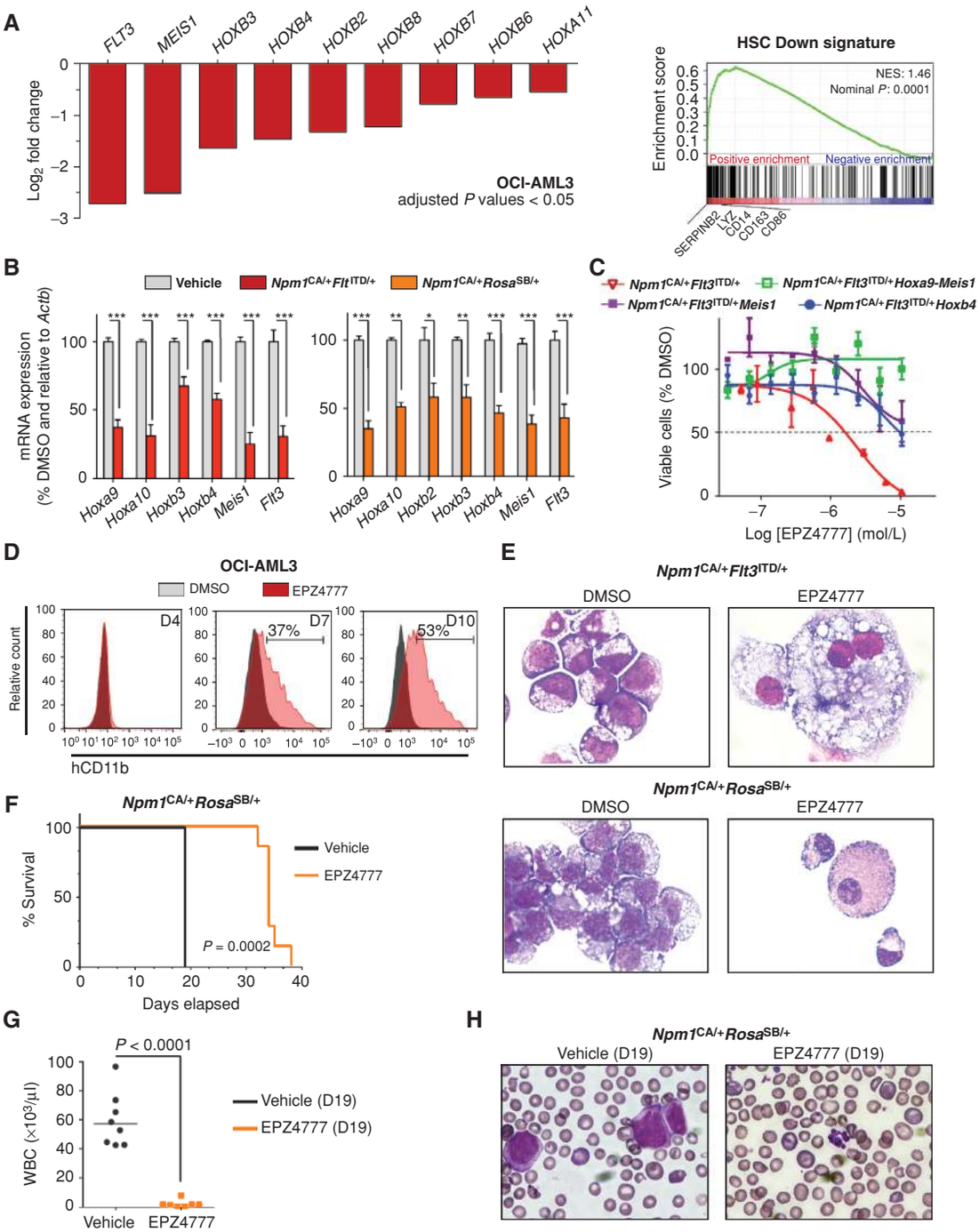

Figure 5. Effects of DOT1L-i on gene expression, cell differentiation, and leukemia-initiating potential in *NPM1*^{mut} AML cells. **A,** left, $\log_2$ fold change of *HOX* genes, *MEIS1*, and *FLT3* between OCI-AML3 cells treated for 7 days with 10 µmol/L EPZ4777 or DMSO vehicle control as assessed by RNA sequencing. Only expressed *HOXA* and *HOXB* cluster genes are shown with a normalized read count of ≥100 reads within the vehicle control, ≥0.5 $\log_2$ fold change, and a *P* value (adjusted for multiple testing) of < 0.05. Right, GSEA of RNA-sequencing data showing enrichment of genes upregulated with EPZ4777 treatment for genes silenced in normal hematopoietic cord blood stem cells. **B,** gene expression in murine *Npm1*$^{CA/+}$*Flt3*$^{ITD/+}$ and *Npm1*$^{CA/+}$*Rosa*$^{SB/+}$ cells assessed on day 7 of EPZ4777 treatment (10 µmol/L) by quantitative PCR. **C,** dose–response curves from cell viability assays after 14 days of EPZ4777 treatment comparing *Npm1*$^{CA/+}$*Flt3*$^{ITD/+}$ cells versus *Npm1*$^{CA/+}$*Flt3*$^{ITD/+}$ cells overexpressing *Hoxb4*, *Meis1*, or *Hoxa9-Meis1*. **D,** cell differentiation upon DOT1L-i (EPZ4777, 10 µmol/L) as determined by flow cytometry for CD11b expression in OCI-AML3 cells (at days 0, 4, and 7 of treatment). **E,** morphologic changes in *Npm1*$^{CA/+}$*Flt3*$^{ITD/+}$ (top) and *Npm1*$^{CA/+}$*Rosa*$^{SB/+}$ (bottom) cells consistent with monocytic differentiation in murine cells after 14 days of EPZ4777 (10 µmol/L) treatment. **F,** Kaplan–Meier survival curve of mice transplanted with pretreated *Npm1*$^{CA/+}$*Rosa*$^{SB/+}$ leukemia cells (vehicle: *n* = 8 mice/group; EPZ4777: *n* = 7 mice/group). White blood cell count (**G**) and morphology (**H**) of mice transplanted with pretreated *Npm1*$^{CA/+}$*Rosa*$^{SB/+}$ leukemia cells on day 19 after transplantation. Data in **A** represent averages of three independently treated replicates per group, data in **B, C,** and **D** represent averages of three independent experiments, each performed in three replicates. Error bars represent the SEM.

Downloaded from http://aacrjournals.org/cancerdiscovery/article-pdf/6/10/1166/1823310/1166.pdf by guest on 26 August 2022

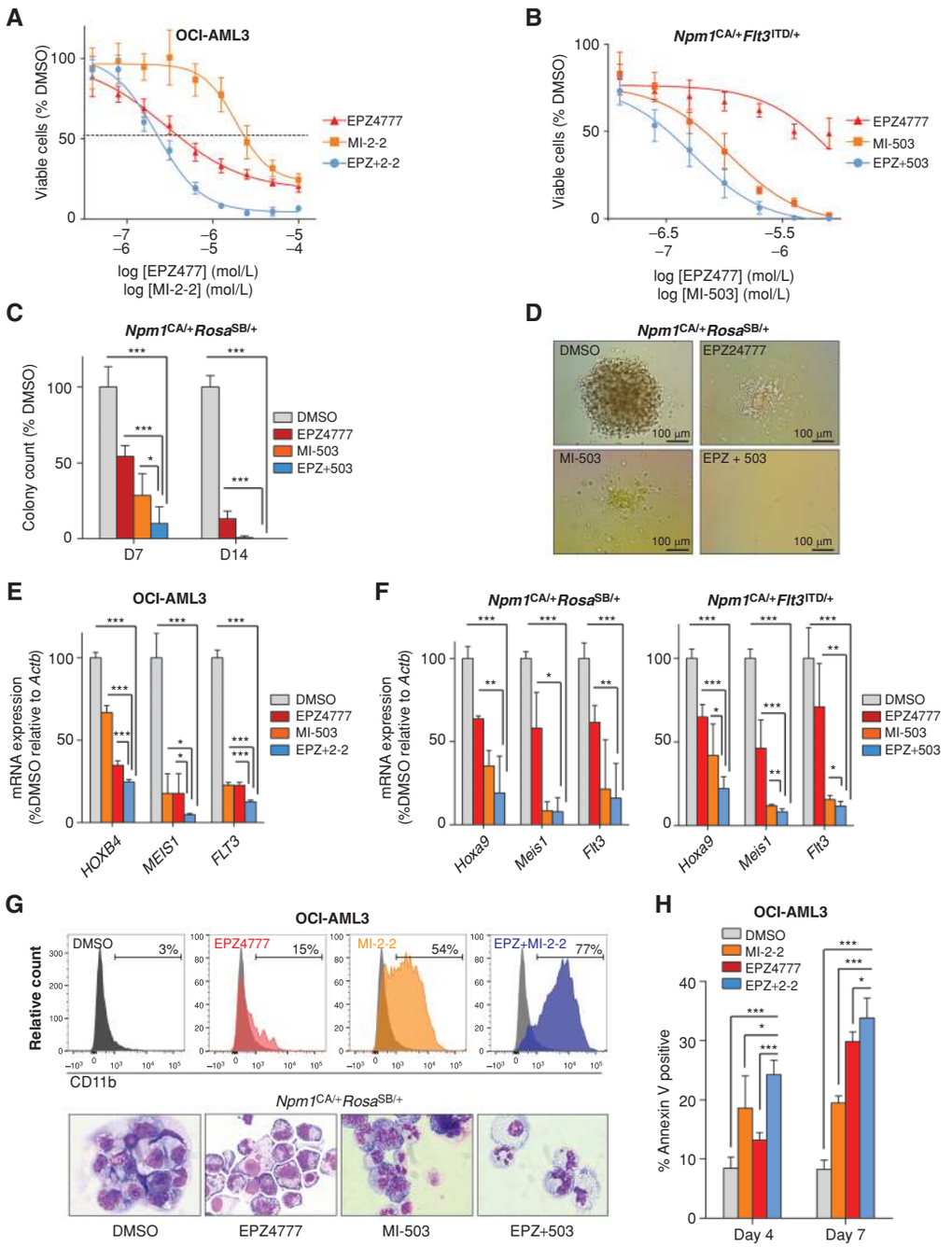

Figure 6. Effects of combinatorial menin–MLL11-i and DOT1L-i in murine and *NPM1*^{mut} leukemia cells. **A,** dose–response curves from cell viability assays of OCI-AML3 cells comparing 7 days of MI-2-2 (12 μmol/L), EPZ4777 (10 μmol/L), and combinatorial EPZ4777 (10 μmol/L) and MI-2-2 (12 μmol/L) (EPZ+2-2) treatment. **B,** dose–response curves from cell viability assays of *Npm1*$^{CA/+}$*Flt3*$^{ITD/+}$ leukemia cells comparing 11 days of MI-503 (2.5 μmol/L), EPZ4777 (10 μmol/L), or combinatorial EPZ4777 (10 μmol/L) and MI-503 (2.5 μmol/L; EPZ + 503) treatment. **C,** comparison of MI-503 (2.5 μmol/L), EPZ4777 (10 μmol/L), and combinatorial MI-503 (2.5 μmol/L) and EPZ4777 (10 μmol/L) treatment of murine *Npm1*$^{CA/+}$*Rosa*$^{SB/+}$ leukemia cells in colony-forming assays assessed on day 7 (D7) and day 14 (D14) of treatment. **D,** representative colony formation of *Npm1*$^{CA/+}$*Rosa*$^{SB/+}$ leukemia cells following 7 days of EPZ4777 (10 μmol/L), MI-503 (2.5 μmol/L), or combinatorial EPZ4777 and MI-503 treatment. **E,** gene expression changes of selected leukemogenic genes in human OCI-AML3 following 4 days of EPZ4777 (10 μmol/L), MI-2-2 (12 μmol/L), or combinatorial EPZ4777 and MI-2-2 treatment as assessed by qPCR. **F,** expression changes of *Hoxa9*, *Meis1*, and *Flt3* in murine *Npm1*$^{CA/+}$*Rosa*$^{SB/+}$ (left) and *Npm1*$^{CA/+}$*Flt3*$^{ITD/+}$ leukemia cells (right) following 4 days of EPZ4777 (10 μmol/L), MI-503 (2.5 μmol/L), or combinatorial EPZ4777 and MI-503 treatment as assessed by qPCR. **G,** cell differentiation of *NPM1*^{mut} leukemia cells as assessed by flow cytometric analysis of CD11b in OCI-AML3 cells (top) and cytology of *Npm1*$^{CA/+}$*Rosa*$^{SB/+}$ leukemia cells (bottom). Representative pictures are shown in the bottom plot, and data were obtained after 4 days of treatment (EPZ4777: 10 μmol/L; MI-2-2: 12 μmol/L; MI-503: 2.5 μmol/L). **H,** apoptosis in OCI-AML3 cells following 4 days of EPZ4777 (10 μmol/L), MI-2-2 (12 μmol/L), or combinatorial EPZ4777 (10 μmol/L) and MI-2-2 (12 μmol/L) treatment as assessed by flow-cytometric staining for Annexin V. Data represent averages of two independent experiments, each performed in three replicates (**A, B, C, E, F, G, H**). Error bars represent the SEM.

Downloaded from http://aacrjournals.org/cancerdiscovery/article-pdf/6/10/1166/1823310/1166.pdf by guest on 26 August 2022

human and the murine *NPM1*^{mut} leukemia using the Chou–Talalay algorithm (ref. 46; Supplementary Fig. S10A and S10B; Supplementary Tables S3 and S4). *Npm1*$^{CA/+}$*Rosa*$^{SB/+}$ leukemia cells that grow only in methylcellulose also exhibited substantially superior suppression of colony-forming potential when treated with both compounds compared with single-drug treatment (Fig. 6C and D).

Gene expression analysis revealed that growth inhibition was preceded by enhanced suppression of leukemogenic gene expression after 4 days of treatment. Although suppression levels of individual *HOX* genes differed across the human and murine *NPM1*^{mut} leukemia models, we found that combinatorial treatment consistently suppressed *MEIS1* transcript levels more than single-drug treatment (Fig. 6E and F). Although EPZ4777 does not reach full suppression of gene expression before 7 days of treatment, we noted that combination treatment resulted in an additional relative reduction of *MEIS1* expression compared with single menin–MLL1-i after only 4 days (OCI-AML3, 73%, P = 0.03; *Npm1*$^{CA/+}$*Flt3*$^{Itd/+}$, 31%, P = 0.001; *Npm1*$^{CA/+}$*Rosa*$^{SB/+}$, 8%, P = 0.89). Similarly, we observed enhanced suppression of *FLT3* in response to combinatorial treatment that reached significance in the OCI-AML3 and the *Npm1*$^{CA/+}$*Flt3*$^{Itd/+}$ cells (Fig. 6E and F). Consistent with these findings, OCI-AML3 cells treated with the combination regimen exhibited less RNA-Polymerase II binding to the *MEIS1* transcriptional start site and gene body region than single-treated cells as assessed by ChIP-PCR (Supplementary Fig. S11), pointing to a direct inhibitory effect of *MEIS1* transcription.

Next, we assessed differentiation following combinatorial menin–MLL1-i and DOT1L-i. In OCI-AML3 cells, differentiation was dramatically more pronounced with both compounds compared with single-drug treatment alone and occurred earlier. After 4 days of treatment, 77% of the cotreated OCI-AML3 cells expressed the monocytic differentiation marker CD11b compared with 54%, 15%, and 3% in the MI-2-2, EPZ4777, or vehicle control–treated cells, respectively (Fig. 6G, top plot). Flow-cytometric data were validated by cyto-morphologic analysis, which revealed more neutrophils or macrophages over blasts with 7 days of combinatorial versus single-drug treatment, particularly pronounced in the murine *Npm1*$^{CA/+}$*Rosa*$^{SB/+}$ cells (Fig. 6G bottom plot and Supplementary Fig. S12). We also detected a significant increase in apoptosis in the OCI-AML3 cells treated with both compounds compared with single treatment alone (Fig. 6H). Overall, these data suggest that combinatorial menin–MLL1-i and DOT1L-i has synergistic therapeutic effects in *NPM1*^{mut} leukemia likely conveyed by enhanced suppression of selected *HOX* genes, *MEIS1*, and *FLT3* as well as induction of differentiation.

Combinatorial Menin–MLL1 and DOT1L Inhibitor Treatment Suppresses Primary AML Cells *In Vitro*

In order to assess the therapeutic potential of combinatorial menin–MLL1-i and DOT1L-i on primary AML patient samples, we used a human stromal cell coculture assay to maintain and treat patient samples *in vitro*. Of 5 *de novo* *NPM1*^{mut} AML patient samples (see patient details in Supplementary Table S5), 1 was not maintainable in culture so the other 4 were used for experiments. Ten days of single-drug treatment with MI-503 (2.5 μmol/L) or EPZ4777 (10 μmol/L) resulted in a profound reduction of viable cell counts compared with DMSO control in all 4 remaining primary AML samples, and we observed an enhanced antiproliferative effect for the combinatorial compared with single-drug treatment in 3 of 4 samples (Fig. 7A). Cell differentiation was also more pronounced with combination therapy (Fig. 7B and Supplementary Fig. S13). These data from primary *NPM1*^{mut} AML patient samples further support single and combinatorial menin–MLL1-i and DOT1L-i as a potentially efficacious therapeutic concept for *NPM1*^{mut} leukemia.

Combinatorial Menin–MLL1-i and DOT1L-i Synergistically Abolishes *NPM1*^{mut} Leukemia-Initiating Potential

Our *in vitro* data showed a synergistic drug effect for simultaneous menin–MLL1-i and DOT1L-i in *NPM1*^{mut} leukemias. To assess the effects of combinatorial drug treatment on leukemia initiating potential, we transplanted equal numbers of viable *Npm1*$^{CA/+}$*Rosa*$^{SB/+}$ leukemia cells pretreated *ex vivo* with drug vehicle, EPZ4777, MI-503, or the combination into sublethally irradiated recipient mice and assessed for leukemia onset and survival. Whereas both EPZ4777 and MI-503 pretreatment led to significantly prolonged survival compared with vehicle control, we observed a significant survival advantage for the drug combination compared with either of the compounds alone (Fig. 7C). Leukemia onset was also significantly delayed as reflected by significantly lower white cell count or CD45.2 engraftment at the time of death from leukemia within the control group (Fig. 7D and Supplementary Fig. S14).

These data confirm that both menin–MLL1-i and DOT1L-i diminish leukemia initiation and indicate that simultaneous inhibition using both compounds shows enhanced effects on leukemia-initiating (stem) cells.

DISCUSSION

Despite being associated with high complete remission rates following standard chemotherapy, less than half of the patients with *NPM1*^{mut} AML achieve long-term disease-free survival due to older age at leukemia onset or concomitant adverse disease factors such as mutations in the *FLT3* gene (9, 14). Research during the last decade has failed to establish mechanism-based targeted therapies specific for *NPM1*^{mut} AML, but described distinctive biological features of this disease such as a *HOX* dominated gene expression signature (4, 6). Efforts to therapeutically target these genes are challenging, as *HOX* and *MEIS1* transcription factors are not amenable to direct pharmacologic inhibition. Lack of knowledge of how aberrant *HOX* expression is driven and maintained during *NPM1*^{mut} leukemic transformation has hindered attempts to indirectly target these genes (3).

Here, we have identified the menin–MLL1 interaction and DOT1L as therapeutic targets that control expression of *HOX* genes, the *HOX* co-factor *MEIS1,* and *FLT3* in *NPM1*^{mut} AML. Using a CRISPR/Cas9 negative selection screen interrogating multiple MLL1 protein domains, we discovered the menin–LEDGF binding site of MLL1 as a dependency in our screen. This is the same region that is critically involved in chromatin binding of the MLL1 complex (19, 20). Also, we detected a strong phenotype for at least one of the sgRNAs targeting the CXXC domain, further pointing to chromatin binding of MLL1 as critically required for *NPM1*^{mut} leukemias (37).

Downloaded from http://aacrjournals.org/cancerdiscovery/article-pdf/6/10/1166/1823310/1166.pdf by guest on 26 August 2022

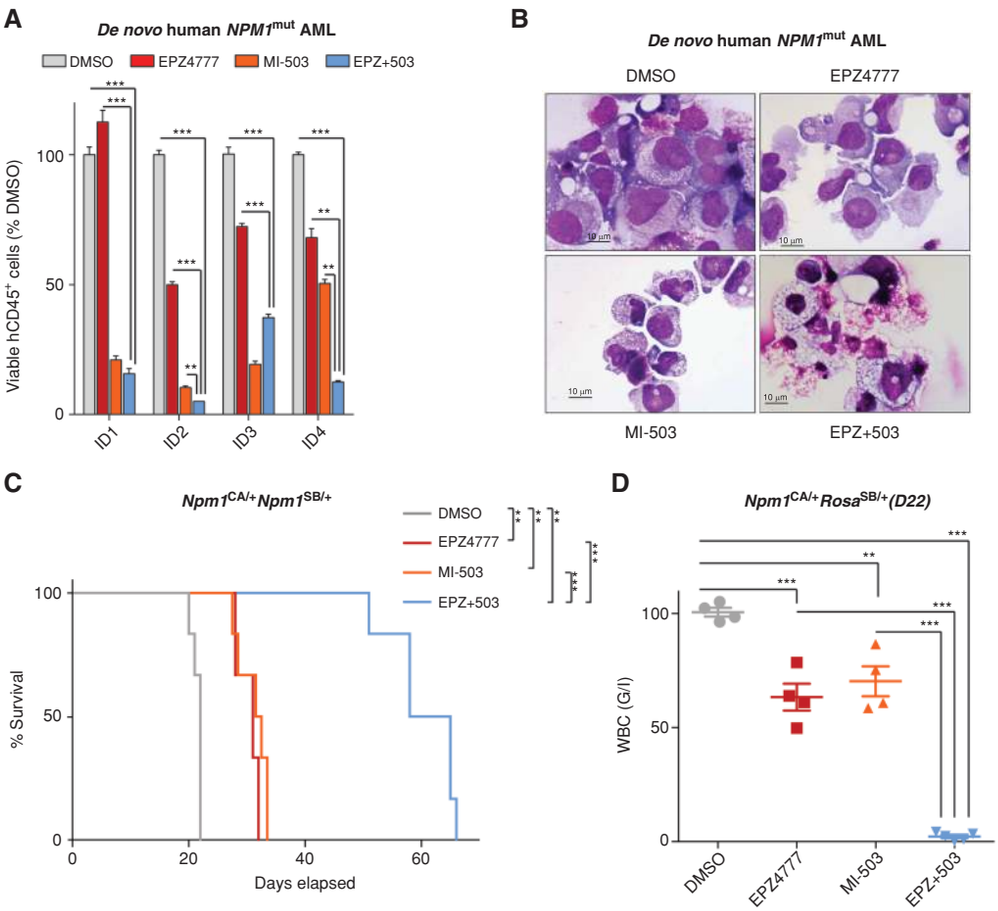

Figure 7. Effects of single and combinatorial menin–MLL1-i and DOT1L-i on primary *NPM1*^{mut} AML patient samples and on leukemia-initiating potential of murine *NPM1*^{mut} leukemias. **A,** viable cell numbers of four independent samples of *de novo NPM1*^{mut} AML treated in coculture assays with DMSO, EPZ4777 (10 μmol/L), MI-503 (2.5 μmol/L), or combinatorial EPZ4777 (10 μmol/L) and MI-503 (2.5 μmol/L). **B,** representative pictures of cytospins from *de novo NPM1*^{mut} AML blasts after 10 days of *in vitro* treatment with vehicle or EPZ4777 (10 μmol/L), MI-503 (2.5 μmol/L), or combinatorial EPZ4777 + MI-503 (10 μmol/L + 2.5 μmol/L) treatment. **C,** Kaplan–Meier survival curve of mice transplanted with pretreated *Npm1*$^{CA/+}$*Rosa*$^{SB/+}$ leukemia cells comparing drug vehicle, EPZ4777, MI-503, or combinatorial EPZ4777 and MI-503 inhibition ($n = 6$ mice/group). **D,** engraftment values in the peripheral blood 22 days after transplantation of pretreated *Npm1*$^{CA/+}$*Rosa*$^{SB/+}$ leukemia cells comparing drug vehicle, EPZ4777, MI-2-2, and combinatorial EPZ4777 and MI-503 inhibition ($n = 4$ mice/group). Bar graphs in **A** represent averages of three replicates assessing one of four independent AML patient samples. Each of the four samples was assessed independently. Error bars represent the SEM.

Furthermore, pharmacologic menin–MLL1-i diminishes menin enrichment at *HOX* and *MEIS1* loci, resulting in dramatic suppression of *HOX* and *MEIS1* expression. Together, these findings strongly support the concept that aberrant *HOX/MEIS1* expression in *NPM1*^{mut} AML is regulated via chromatin binding of the menin–WT-MLL1 complex. Whether *HOX* gene activation is a direct consequence of MLL1 binding to chromatin itself or dependent on other proteins that are indirectly recruited to chromatin via MLL1 remains to be determined. It is of interest to note that none of the sgRNAs targeting the C-terminal SET domain of *MLL1* containing the H3K4 methyltransferase activity exhibited any significant phenotype. These data are in line with a recent study on MLL1-fusion leukemias where selective inactivation of the SET domain did not alter transcription of *HOX* genes or transformation potential (47), but future studies will need to assess the importance of this domain with more detailed experiments. In addition, we found no evidence that the SET domain of MLL2, the other MLL family member interacting with menin, is involved in *NPM1*^{mut} leukemogenesis.

We have also shown that DOT1L is another chromatin modifier important for the control of *HOX* gene expression in *NPM1*^{mut} leukemias. We show that not only *HOXA* and *MEIS1* but also *HOXB* expression is dependent on DOT1L in murine hematopoietic stem-cell progenitor cells (LSK cells) and the high expression levels that are associated with higher states of H3K79 methylation at those gene loci point to an important role for DOT1L. Although there is evidence that DOT1L is misdirected to *HOXA* cluster loci in MLL1-fusion leukemias via the fusion partner protein (30), the data presented here suggest that regulatory mechanisms that normally control *HOX* gene expression in hematopoietic cells remain critical in *NPM1*^{mut} AML. Just as we found with inhibition of the menin–MLL1 interaction, we found that pharmacologic DOT1L-i resulted in *HOX* downregulation, cell growth inhibition, and profound differentiation of *NPM1*^{mut} AML blasts. These data therefore

Downloaded from http://aacrjournals.org/cancerdiscovery/article-pdf/6/10/1166/1823310/1166.pdf by guest on 26 August 2022

extend the rationale for therapeutic DOT1L-i from MLL1-fusion leukemias to the much more prevalent *NPM1*^{mut} AML and prompt further study as to the mechanisms by which *HOX* genes are controlled in various genetics subtypes of AML.

A particularly striking finding was that the profound downregulation of *MEIS1* following menin–MLL1-i was accompanied by almost complete suppression of *FLT3* expression. *FLT3* has been previously shown to be a transcriptional target of *MEIS1* (38), and thus we believe that this suppression is most likely conveyed via *MEIS1* rather than a direct effect caused by MLL1 or DOT1L-i. This observation might be of particular therapeutic importance as up to 66% of *NPM1*^{mut} AMLs harbor concomitant activating *FLT3* mutations associated with adverse outcome (8, 10, 11). Thus, menin–MLL1-i may be particularly attractive for patients exhibiting the unfavorable *NPM1*^{mut} *FLT3*-ITD genotype.

Whereas our data provide evidence that *HOX* genes and *MEIS1* in *NPM1*^{mut} leukemias are regulated on a chromatin level via MLL1 and DOT1L, the specific role of the mutant NPM1 protein with regard to *HOX* and *MEIS1* regulation remains elusive. However, the strong association between *HOX* expression in human *NPM1*^{mut} AML or genetic knock-in models of *NPM1*^{mut} leukemia in mice together with the above-presented data suggests that the mutant NPM1 protein acts upstream of menin–MLL1 and DOT1L to deregulate gene expression, at least partially analogous to the functions of MLL1-fusion proteins in *MLL*-rearranged leukemias. The strong oncogenic transformation potential of *HOX* genes in general suggests that these genes are likely required for *NPM1*^{mut}-driven leukemogenesis. Whereas formal proof of this view was lacking, our data provide strong support for this concept, as exogenous overexpression of selected *HOX* genes rescues antiproliferative effects of both DOT1L and menin–MLL1 inhibitors. We further show that combinatorial inhibition of menin–MLL1 and DOT1L has enhanced on-target activity as reflected by more profound *HOX* and *MEIS1* suppression. These changes result in a synergistic antiproliferative and boosted differentiation effect, suggesting that therapeutic *HOX* targeting ultimately releases the differentiation block of *NPM1*^{mut} AML blasts.

The availability of menin–MLL1 and DOT1L inhibitors should enable relatively quick translation of our findings into clinical testing. However, future studies will determine whether the potent antileukemic activity can be best harnessed when introduced into current standard chemotherapy regimens, thereby overcoming possible context-specific escape mechanisms that are frequently observed in AML. A proof-of-principle study on leukemia cell lines already demonstrated drug synergism of EPZ-5676 with standard chemotherapeutic agents *in vitro* (48). Another interesting combination partner might be dactinomycin that directly inhibits transcriptional elongation by inhibition of RNA polymerases and was reported to have activity against *NPM1*^{mut} leukemia in an anecdotal report on a single patient (49).

In summary, our data show that *NPM1*^{mut} leukemogenesis is dependent on *HOX* and *MEIS1* expression, which is controlled by specific chromatin-regulatory complexes. We further demonstrate that these genes are therapeutically targetable via the menin–MLL1 interaction and the H3K79 methyltransferase DOT1L. Small-molecule inhibition of these two histone modifiers releases the differentiation block of *NPM1*^{mut} leukemic blasts. Both compounds as single agents or in combination represent novel and possibly less toxic therapeutic opportunities for the relatively common *NPM1*^{mut} leukemias and represent an attractive concept particularly for patients with the prognostically adverse genotype with concomitant *FLT3*-ITD and the difficult-to-treat elderly population.

METHODS

Cell Culture and Cell Lines

The AML cell lines OCI-AML3, OCI-AML2, SET2, MOLM13, and HL60, as well as 293T cells and Hs27 cells, were maintained under standard conditions. Cell line authentication testing (ATCC) was performed between March and November 2013 and verified identity and purity for all human AML cell lines used in this study. The murine leukemia models *Npm1*$^{CA/+}$*Flt3*$^{ITD/+}$ and *Npm1*$^{CA/+}$*Rosa*$^{SB/+}$ were described previously (39, 40), and cells were cultured as previously described (29). With regard to the *Npm1*$^{CA/+}$*Rosa*$^{SB/+}$ model, leukemias with two different sleeping beauty integration sites were used (A: target gene: *Csf2*, position: 54064482, and target gene: *Mll1*, position: 44649906; B: target gene: *Csf2*, position: 54250117; genomic positions are as per Ensemble assembly NCBIm37) for all *in vitro* studies. Experiments were performed using A, as these cells were found to have a slightly higher colony-forming potential *in vitro*. Confirmation of the results was then performed with B.

CRISPR/Cas9 Screening

The pCW-Cas9 expression construct and the pLKO5.sgRNA.EFS.GFP vector were purchased from Addgene (#50661 and #57822). All sgRNAs in this study were designed using the Zhang laboratory's CRISPR design webpage at MIT, and sequences are listed in Supplementary Tables S1 and S2. OCI-AML3-pCW-Cas9 cells were derived by retroviral transduction of OCI-AML3 cells with pCW-Cas9, followed by puromycin selection. Cells were plated in methylcellulose to obtain single-cell–derived clones, and screened for Cas9 expression by immunoblotting using an anti-flag antibody. The *MLL1* and *MLL2* domain screen was performed in duplicate and repeated with two independent clones. Three days following sgRNA transduction, Cas9 was induced and GFP$^+$/GFP$^-$ ratio determined every 3 days for 15 days as described (34). For more details, see Supplementary Methods.

In Vitro *Studies*

RNA purification, cDNA synthesis, qRT-PCR, immunoblotting, ChIP-PCR, flow cytometry, retroviral overexpression, and *in vitro* drug treatment in colony-forming or cell viability assays were performed using standard procedures. A detailed description is provided in the supplementary material. Drug synergy was assessed in viability assays comparing single versus constant ratios of combinatorial drug treatment using the Chou–Talalay method (46) and is also described in detail in the supplementary material.

RNA Sequencing and Analysis

For gene expression analysis, biological triplicates of OCI-AML3 cells were treated for 7 days with DMSO or 10 μmol/L EPZ4777. ERCC synthetic spike-in controls were added to cell lysis buffer of each sample based on cell number and prior to RNA isolation. For fusion detection, triplicates of untreated OCI-AML2 cells were harvested for RNA purification. See Supplementary Methods for RNA purification, library construction, and sequencing analysis. Data were made publicly available at the Gene Expression Omnibus (accession code: GSE85107).

OCI-AML3 Xenograft Model

For *in vivo* treatment experiments, 7-to-10-week-old female NSG mice were injected via tail vein with 5×10^6 OCI-AML3 cells. Animals

Downloaded from http://aacrjournals.org/cancerdiscovery/article-pdf/6/10/1166/1823310/1166.pdf by guest on 26 August 2022

were randomized to vehicle (25% DMSO, 25% PEG 400, and 50% normal saline) or MI-503 (50 mg/kg bid IP) starting on day 5 after transplantation. For assessment of leukemia burden, mice were sacrificed between 7 and 12 days of drug treatment and harvested bone marrow cells assessed for human CD45 expression using flow cytometry. For gene expression analysis, RNA was isolated from MACS-sorted human CD45$^+$ cells. For survival analysis, treatment was initiated on day 7 for 26 days in total with a 3-day treatment break to allow partial recovery from local irritation at the injection sites. Mice were monitored daily for clinical symptoms. Moribund animals were euthanized when they displayed signs of terminal leukemic disease. All mouse experiments were approved by the Institutional Animal Care and Use Committee at Memorial Sloan Kettering Cancer Center.

Murine Bone Marrow Transplantation Models

In Vivo *Treatment Studies* 1×10^6 *Npm1*$^{CA/+}$*Rosa*$^{SB/+}$ (model A) secondary leukemia cells, harvested from moribund animals, were transplanted into sublethally irradiated (200 cGy) female NSG mice via tail vein injection. Mice were randomized to vehicle or MI-503 (50 mg/kg, bid, 10 days IP), and treatment initiated 7 days after transplantation.

Ex Vivo *Treatment Studies* (a) *Npm1*$^{CA/+}$*Flt3*$^{ITD/+}$ and *Npm1*$^{CA/+}$*Rosa*$^{SB/+}$ (model A) secondary leukemia cells were treated with DMSO or EPZ4777 (10 μmol/L) for 11 days in tissue culture or (b) *Npm1*$^{CA/+}$*Rosa*$^{SB/+}$ secondary leukemia cells for 10 days with either DMSO, EPZ4777 (10 μmol/L), or 4 days of MI-503 (2.5 μmol/L) plus 6 days of DMSO or 6 days of EPZ4777 (10 μmol/L) plus 4 days of combinatorial EPZ4777 (10 μmol/L) + MI-503 (2.5 μmol/L). Pretreated viable cells (1×10^6) of each group were then transplanted into sublethally irradiated female NSG (*Npm1*$^{CA/+}$*Rosa*$^{SB/+}$) or C57BL/6J (irradiated with 600cGy; *Npm1*$^{CA/+}$*Flt3*$^{ITD/+}$) recipient animals.

Human AML Coculture Assay

The coculture treatment assay of primary human AML samples was performed as previously reported (50) and is described in the supplementary material. Human AML samples were obtained under Institutional Review Board–approved protocols from patients treated at Memorial Sloan Kettering Cancer Center following written informed consent.

Data Analysis and Statistical Methods

Statistical test computations were performed using Graph Pad Prism (v6). Statistical significance for the *in vitro* assays was calculated using the Student *t* test. Survival analysis was estimated using the Kaplan–Meier method, and *P* values were calculated using the log-rank test. *P* values were displayed as follows: *, $P < 0.05$; **, $P < 0.005$; ***, $P < 0.0005$. *In vitro* assessment of menin–MLL1-i in the *NPM1*^{mut} AML models was performed in at least two independent experiments each performed in three replicates using one of the two menin–MLL1 inhibitors (MI-2-2 or MI-503). In addition, results for most experiments were confirmed once with the other menin–MLL1 inhibitor. *In vitro* studies related to DOT1L-i were performed in three independent experiments each performed in three replicates.

Disclosure of Potential Conflicts of Interest

J.E. Bradner is President at Novartis Institute of BioMedical Research. G.S. Vassiliou reports receiving a commercial research grant from Celgene and is a consultant/advisory board member for Kymab Ltd. S.A. Armstrong is a consultant/advisory board member for Epizyme, Inc., and Vitae Pharmaceuticals. No potential conflicts of interest were disclosed by the other authors.

Authors' Contributions

Conception and design: M.W.M. Kühn, C.-W. Chen, S.A. Armstrong
Development of methodology: M.W.M. Kühn, Z. Feng, C.-W. Chen, A.J. Deshpande, M. Cusan, J.E. Bradner, S.A. Armstrong
Acquisition of data (provided animals, acquired and managed patients, provided facilities, etc.): M.W.M. Kühn, E. Song, A. Mupo, C. Grove, E. de Stanchina, S.A. Armstrong
Analysis and interpretation of data (e.g., statistical analysis, biostatistics, computational analysis): M.W.M. Kühn, E. Song, A. Sinha, N. Farnoud, R. Koche, S.A. Armstrong
Writing, review, and/or revision of the manuscript: M.W.M. Kühn, N. Farnoud, J.E. Bradner, S.A. Armstrong
Administrative, technical, or material support (i.e., reporting or organizing data, constructing databases): Z. Feng, T. Hoshii, S.A. Armstrong
Study supervision: S.A. Armstrong
Other [contributed mouse Npm1c-driven leukemias (live cells)]: G.S. Vassiliou

Acknowledgments

We thank members of the Armstrong Laboratory for helpful comments on the article; Rowena Eng, Huiyong Zhao, and Michael Hadler for excellent technical assistance; and Olga Guryanova and Ross Levine for the SET2 and OCI-AML2 cell lines.

Grant Support

This study was supported by grants (to S.A. Armstrong) from the NIH (CA66996, CA140575, and CA176745) and the Leukemia and Lymphoma Society. E. de Stanchina was supported by an NIH grant (P30 CA008748). M.W.M. Kühn was supported by the German Research Foundation (DFG; KU 2688/1-1).

The costs of publication of this article were defrayed in part by the payment of page charges. This article must therefore be hereby marked *advertisement* in accordance with 18 U.S.C. Section 1734 solely to indicate this fact.

Received February 24, 2016; revised August 10, 2016; accepted August 11, 2016; published OnlineFirst August 17, 2016.

REFERENCES

1. Sauvageau G, Lansdorp PM, Eaves CJ, Hogge DE, Dragowska WH, Reid DS, et al. Differential expression of homeobox genes in functionally distinct CD34+ subpopulations of human bone marrow cells. Proc Natl Acad Sci U S A 1994;91:12223–7.
2. Giampaolo A, Sterpetti P, Bulgarini D, Samoggia P, Pelosi E, Valtieri M, et al. Key functional role and lineage-specific expression of selected HOXB genes in purified hematopoietic progenitor differentiation. Blood 1994;84:3637–47.
3. Alharbi RA, Pettengell R, Pandha HS, Morgan R. The role of HOX genes in normal hematopoiesis and acute leukemia. Leukemia 2013;27:1000–8.
4. Spencer DH, Young MA, Lamprecht TL, Helton NM, Fulton R, O'Laughlin M, et al. Epigenomic analysis of the HOX gene loci reveals mechanisms that may control canonical expression patterns in AML and normal hematopoietic cells. Leukemia 2015;29:1279–89.
5. Argiropoulos B, Humphries RK. Hox genes in hematopoiesis and leukemogenesis. Oncogene 2007;26:6766–76.
6. Mullighan CG, Kennedy A, Zhou X, Radtke I, Phillips LA, Shurtleff SA, et al. Pediatric acute myeloid leukemia with NPM1 mutations is characterized by a gene expression profile with dysregulated HOX gene expression distinct from MLL-rearranged leukemias. Leukemia 2007;21:2000–9.
7. Alcalay M, Tiacci E, Bergomas R, Bigerna B, Venturini E, Minardi SP, et al. Acute myeloid leukemia bearing cytoplasmic nucleophosmin (NPMc+ AML) shows a distinct gene expression profile characterized by up-regulation of genes involved in stem-cell maintenance. Blood 2005;106:899–902.
8. Falini B, Mecucci C, Tiacci E, Alcalay M, Rosati R, Pasqualucci L, et al. Cytoplasmic nucleophosmin in acute myelogenous leukemia with a normal karyotype. N Engl J Med 2005;352:254–66.

Downloaded from http://aacrjournals.org/cancerdiscovery/article-pdf/6/10/1166/1823310/1166.pdf by guest on 26 August 2022

9. Schnittger S, Schoch C, Kern W, Mecucci C, Tschulik C, Martelli MF, et al. Nucleophosmin gene mutations are predictors of favorable prognosis in acute myelogenous leukemia with a normal karyotype. Blood 2005;106:3733–9.
10. Ivey A, Hills RK, Simpson MA, Jovanovic JV, Gilkes A, Grech A, et al. Assessment of minimal residual disease in standard-risk AML. N Engl J Med 2016;374:422–33.
11. Schlenk RF, Dohner K, Krauter J, Frohling S, Corbacioglu A, Bullinger L, et al. Mutations and treatment outcome in cytogenetically normal acute myeloid leukemia. N Engl J Med 2008;358:1909–18.
12. Verhaak RG, Goudswaard CS, van Putten W, Bijl MA, Sanders MA, Hugens W, et al. Mutations in nucleophosmin (NPM1) in acute myeloid leukemia (AML): Association with other gene abnormalities and previously established gene expression signatures and their favorable prognostic significance. Blood 2005;106:3747–54.
13. Daver N, Cortes J, Ravandi F, Patel KP, Burger JA, Konopleva M, et al. Secondary mutations as mediators of resistance to targeted therapy in leukemia. Blood 2015;125:3236–45.
14. Ostronoff F, Othus M, Lazenby M, Estey E, Appelbaum FR, Evans A, et al. Prognostic significance of NPM1 mutations in the absence of FLT3-internal tandem duplication in older patients with acute myeloid leukemia: a SWOG and UK National Cancer Research Institute/Medical Research Council report. J Clin Oncol 2015;33:1157–64.
15. Federici L, Falini B. Nucleophosmin mutations in acute myeloid leukemia: A tale of protein unfolding and mislocalization. Protein Sci 2013;22:545–56.
16. Okuwaki M, Matsumoto K, Tsujimoto M, Nagata K. Function of nucleophosmin/B23, a nucleolar acidic protein, as a histone chaperone. FEBS Lett 2001;506:272–6.
17. Krivtsov AV, Armstrong SA. MLL translocations, histone modifications and leukaemia stem-cell development. Nat Rev Cancer 2007;7:823–33.
18. Krivtsov AV, Twomey D, Feng Z, Stubbs MC, Wang Y, Faber J, et al. Transformation from committed progenitor to leukaemia stem cell initiated by MLL-AF9. Nature 2006;442:818–22.
19. Yokoyama A, Cleary ML. Menin critically links MLL proteins with LEDGF on cancer-associated target genes. Cancer Cell 2008;14:36–46.
20. Yokoyama A, Somervaille TC, Smith KS, Rozenblatt-Rosen O, Meyerson M, Cleary ML. The menin tumor suppressor protein is an essential oncogenic cofactor for MLL-associated leukemogenesis. Cell 2005;123:207–18.
21. Shi A, Murai MJ, He S, Lund G, Hartley T, Purohit T, et al. Structural insights into inhibition of the bivalent menin-MLL interaction by small molecules in leukemia. Blood 2012;120:4461–9.
22. Borkin D, He S, Miao H, Kempinska K, Pollock J, Chase J, et al. Pharmacologic inhibition of the Menin-MLL interaction blocks progression of MLL leukemia in vivo. Cancer Cell 2015;27:589–602.
23. Yu BD, Hess JL, Horning SE, Brown GA, Korsmeyer SJ. Altered Hox expression and segmental identity in Mll-mutant mice. Nature 1995;378:505–8.
24. Ernst P, Fisher JK, Avery W, Wade S, Foy D, Korsmeyer SJ. Definitive hematopoiesis requires the mixed-lineage leukemia gene. Dev Cell 2004;6:437–43.
25. Chen YX, Yan J, Keeshan K, Tubbs AT, Wang H, Silva A, et al. The tumor suppressor menin regulates hematopoiesis and myeloid transformation by influencing Hox gene expression. Proc Natl Acad Sci U S A 2006;103:1018–23.
26. Novotny E, Compton S, Liu PP, Collins FS, Chandrasekharappa SC. In vitro hematopoietic differentiation of mouse embryonic stem cells requires the tumor suppressor menin and is mediated by Hoxa9. Mech Dev 2009;126:517–22.
27. Bernt KM, Zhu N, Sinha AU, Vempati S, Faber J, Krivtsov AV, et al. MLL-rearranged leukemia is dependent on aberrant H3K79 methylation by DOT1L. Cancer Cell 2011;20:66–78.
28. Deshpande AJ, Deshpande A, Sinha AU, Chen L, Chang J, Cihan A, et al. AF10 regulates progressive H3K79 methylation and HOX gene expression in diverse AML subtypes. Cancer Cell 2014;26:896–908.
29. Chen CW, Koche RP, Sinha AU, Deshpande AJ, Zhu N, Eng R, et al. DOT1L inhibits SIRT1-mediated epigenetic silencing to maintain leukemic gene expression in MLL-rearranged leukemia. Nat Med 2015;21:335–43.
30. Deshpande AJ, Bradner J, Armstrong SA. Chromatin modifications as therapeutic targets in MLL-rearranged leukemia. Trends Immunol 2012;33:563–70.
31. Daigle SR, Olhava EJ, Therkelsen CA, Basavapathruni A, Jin L, Boriack-Sjodin PA, et al. Potent inhibition of DOT1L as treatment of MLL-fusion leukemia. Blood 2013;122:1017–25.
32. Daigle SR, Olhava EJ, Therkelsen CA, Majer CR, Sneeringer CJ, Song J, et al. Selective killing of mixed lineage leukemia cells by a potent small-molecule DOT1L inhibitor. Cancer Cell 2011;20:53–65.
33. Stein EM, Tallman MS. Mixed lineage rearranged leukaemia: Pathogenesis and targeting DOT1L. Curr Opin Hematol 2015;22:92–6.
34. Shi J, Wang E, Milazzo JP, Wang Z, Kinney JB, Vakoc CR. Discovery of cancer drug targets by CRISPR-Cas9 screening of protein domains. Nat Biotechnol 2015;33:661–7.
35. Huang J, Gurung B, Wan B, Matkar S, Veniaminova NA, Wan K, et al. The same pocket in menin binds both MLL and JUND but has opposite effects on transcription. Nature 2012;482:542–6.
36. Cierpicki T, Risner LE, Grembecka J, Lukasik SM, Popovic R, Omonkowska M, et al. Structure of the MLL CXXC domain-DNA complex and its functional role in MLL-AF9 leukemia. Nat Struct Mol Biol 2010;17:62–8.
37. Lee JH, Tate CM, You JS, Skalnik DG. Identification and characterization of the human Set1B histone H3-Lys4 methyltransferase complex. J Biol Chem 2007;282:13419–28.
38. Wang GG, Pasillas MP, Kamps MP. Meis1 programs transcription of FLT3 and cancer stem cell character, using a mechanism that requires interaction with Pbx and a novel function of the Meis1 C-terminus. Blood 2005;106:254–64.
39. Vassiliou GS, Cooper JL, Rad R, Li J, Rice S, Uren A, et al. Mutant nucleophosmin and cooperating pathways drive leukemia initiation and progression in mice. Nat Genet 2011;43:470–5.
40. Mupo A, Celani L, Dovey O, Cooper JL, Grove C, Rad R, et al. A powerful molecular synergy between mutant Nucleophosmin and Flt3-ITD drives acute myeloid leukemia in mice. Leukemia 2013;27:1917–20.
41. Grembecka J, He S, Shi A, Purohit T, Muntean AG, Sorenson RJ, et al. Menin-MLL1 inhibitors reverse oncogenic activity of MLL fusion proteins in leukemia. Nat Chem Biol 2012;8:277–84.
42. Loven J, Orlando DA, Sigova AA, Lin CY, Rahl PB, Burge CB, et al. Revisiting global gene expression analysis. Cell 2012;151:476–82.
43. Ribeiro AF, Pratcorona M, Erpelinck-Verschueren C, Rockova V, Sanders M, Abbas S, et al. Mutant DNMT3A: A marker of poor prognosis in acute myeloid leukemia. Blood 2012;119:5824–31.
44. Gaidzik VI, Schlenk RF, Paschka P, Stolzle A, Spath D, Kuendgen A, et al. Clinical impact of DNMT3A mutations in younger adult patients with acute myeloid leukemia: Results of the AML Study Group (AMLSG). Blood 2013;121:4769–77.
45. Deshpande AJ, Chen L, Fazio M, Sinha AU, Bernt KM, Banka D, et al. Leukemic transformation by the MLL-AF6 fusion oncogene requires the H3K79 methyltransferase Dot1l. Blood 2013;121:2533–41.
46. Chou TC. Theoretical basis, experimental design, and computerized simulation of synergism and antagonism in drug combination studies. Pharmacol Rev 2006;58:621–81.
47. Mishra BP, Zaffuto KM, Artinger EL, Org T, Mikkola HK, Cheng C, et al. The histone methyltransferase activity of MLL1 is dispensable for hematopoiesis and leukemogenesis. Cell Rep 2014;7:1239–47.
48. Klaus CR, Iwanowicz D, Johnston D, Campbell CA, Smith JJ, Moyer MP, et al. DOT1L inhibitor EPZ-5676 displays synergistic antiproliferative activity in combination with standard of care drugs and hypomethylating agents in MLL-rearranged leukemia cells. J Pharmacol Exp Ther 2014;350:646–56.
49. Falini B, Brunetti L, Martelli MP. Dactinomycin in NPM1-mutated acute myeloid leukemia. N Engl J Med 2015;373:1180–2.
50. Kühn MWM, Hadler MJ, Daigle SR, Koche RP, Krivtsov AV, Olhava EJ, et al. MLL partial tandem duplication leukemia cells are sensitive to small molecule DOT1L inhibition. Haematologica 2015;100:e190–3.

Downloaded from http://aacrjournals.org/cancerdiscovery/article-pdf/6/10/1166/1823310/1166.pdf by guest on 26 August 2022